



A New Era in Computational Pathology: A Survey on Foundation and Vision-Language Models

Dibaloke Chanda , *Graduate Student Member, IEEE*,

Milan Aryal ,

Nasim Yahya Soltani , *Member, IEEE*

Masoud Ganji, *Fellow, CAP*

Abstract—Recent advances in deep learning have completely transformed the domain of computational pathology (CPATH). More specifically, it has altered the diagnostic workflow of pathologists by integrating foundation models (FMs) and vision-language models (VLMs) in their assessment and decision-making process. The limitations of existing deep learning approaches in CPATH can be overcome by FMs through learning a representation space that can be adapted to a wide variety of downstream tasks without explicit supervision. Deploying VLMs allow pathology reports written in natural language be used as rich semantic information sources to improve existing models as well as generate predictions in natural language form. In this survey, a holistic and systematic overview of recent innovations in FMs and VLMs in CPATH is presented. Furthermore, the tools, datasets and training schemes for these models are summarized in addition to categorizing them into distinct groups. This extensive survey highlights the current trends in CPATH and its possible revolution through the use of FMs and VLMs in the future.

Index Terms—Computational pathology, foundation models, multi-modal, vision-language models.

I. INTRODUCTION

In recent years there has been a surge of artificial intelligence (AI)-based approaches [1]–[19] in computational pathology (CPATH) owing to wide adoption of digital slide scanners. In fact, large-scale curation and annotation [20], [21] of whole slide images (WSIs) has ensured adequate data for training of these AI-based models. The goal of generating such AI-based models is to automate and expedite the diagnosis and prognosis process of CPATH. Traditional diagnosis process in CPATH is time-consuming and requires experts with extensive domain knowledge. In addition, the wide range of cancer types and grades as well as the heterogeneity among diagnosis/prognosis tasks, makes it challenging to come up with a unified general approach.

Several research studies have addressed the issue with a unified approach and among the proposed methods, foundation models (FMs) have gained a lot of attention in recent years [22]–[42]. More specifically, FMs leverage self-supervised learning (SSL) [43] schemes to learn a rich representation in a task-agnostic manner. Owing to self-supervised pre-training (SSPT), FMs do not require large-scale annotated data which is hard to come by in CPATH. Furthermore, these models can be trained with a diverse selection of datasets containing tissue samples from different organs and associated with different

cancer types, as well as scanner types. Certain research works focus on making sure this diversity is present in the pre-training dataset [26], [29]. As a result, the resultant pre-trained model can easily be utilized in a wide range of downstream tasks while maintaining robustness to extreme variation in tissue samples.

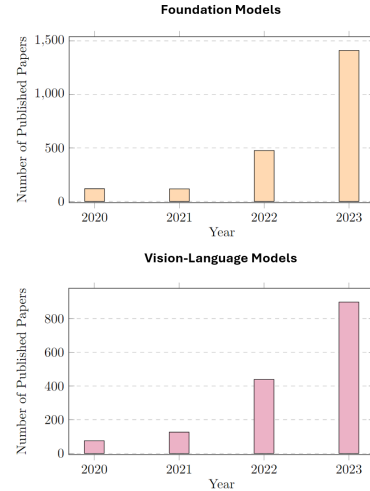


Fig. 1. Number of publications for FMs and VLMs in pathology (from Google Scholar). The search keywords include “vision-language” + “pathology” for VLMs statistics and “foundation models”+ “pathology” for FMs statistics.

The impact of FMs in CPATH can be amplified by integrating the power of vision-language models (VLMs) [44]. More specifically, VLMs have surged in popularity after the introduction of contrastive language-image pre-training (CLIP) model by OpenAI [45]. Pathology reports, books, educational videos, etc. are rich sources of semantic information that can be utilized by VLMs to significantly boost the performance. This is not typically possible with vision-only models. When deployed in conjunction with FMs, they can perform as AI-based pathologists capable of performing a vast array of tasks as evidenced by recent literature [37]. Even though CPATH is a specialized area of study in the medical field, there is a large increase in the number of publications focusing on FMs and VLMs in pathology as shown in Fig. 1 demonstrating a dominant future direction of this field.

To appreciate the full impact of FMs and VLMs in CPATH, the major challenges in CPATH are outlined in Fig. 2. In addition, the way FMs and VLMs address these challenges

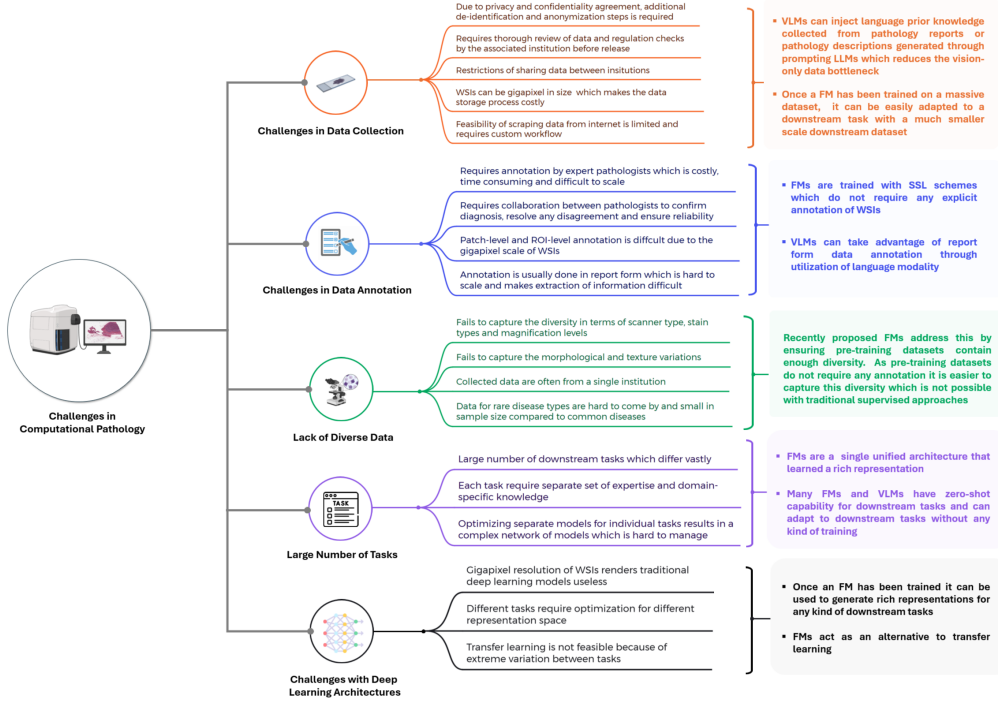


Fig. 2. Outline of major challenges in CPath. Several causes and consequences for each challenge are outlined in addition to how FMs and VLMs address these challenges.

is also mentioned.

A. Scope of the Review

In this review, the main emphasis is put on the application of FMs and VLMs in CPath, especially the details of their architectures and training schemes. Note that these two categories are not mutually exclusive, meaning that some research articles belong to both categories which are vision-language foundation models (VLFMs). In addition, details of multi-modal datasets are summarized with a focus on vision and language as the modalities. Several self-imposed rules and

- 2) Secondly, only vision-language models are included and articles that use other modalities along with vision are excluded. As an example, along with vision, transcriptomics [47] can be used to address pathology tasks. However, such papers are excluded to maintain the scope.
- 3) Both peer-reviewed articles and pre-print articles are included in the survey. Among the peer-reviewed articles, a significant number of articles are published in top-tier journals and conferences as shown in Table I.

B. Contribution and Organization

In the past few years, quite a few review articles [1]–[19] have been published focusing on CPath. Most of these articles provide a review of the application of deep learning as a whole rather than focusing on a specific subtopic. There are handful of papers that focus on specific architecture like MIL [18], graph-based models [17], [48], transformer-based models [10], [13], LLMs [19], etc. The contributions of this review article are summarized below:

- 1) To the best of our knowledge, this is the first review article to summarize recent advances (most articles from 2023-2024) in FMs and VLMs (Section III and IV). The closest peer-reviewed survey article [8] mostly provides a high-level overview without going into the details of FMs.
- 2) An exhaustive list of multi-modal datasets (Section II) in CPath that are being used or can be used in vision-language research are outlined.
- 3) Given the diverse datasets and architectures, descriptions for individual research are provided in tabular format (Ta-

TABLE I
NUMBER OF SURVEYED ARTICLES PUBLISHED IN TOP JOURNALS AND CONFERENCES WITHIN 2021-2024

Journal/Conference Venue	Counts
Nature/Nature Medicine	6
CVPR	8
NeurIPS	2
ECCV/WACV/ICCV	5
MICCAI	5
AAAI	2
Elsevier/Springer	6

restrictions were used as guidelines throughout the review to ensure the scope of the paper is maintained.

- 1) First, articles that focus solely on pathology are included. So, and articles with a focus on other areas of the biomedical domain are excluded. As an example, articles like BiomedCLIP [46] with pathology as a subsection of the research are not included in this review paper.

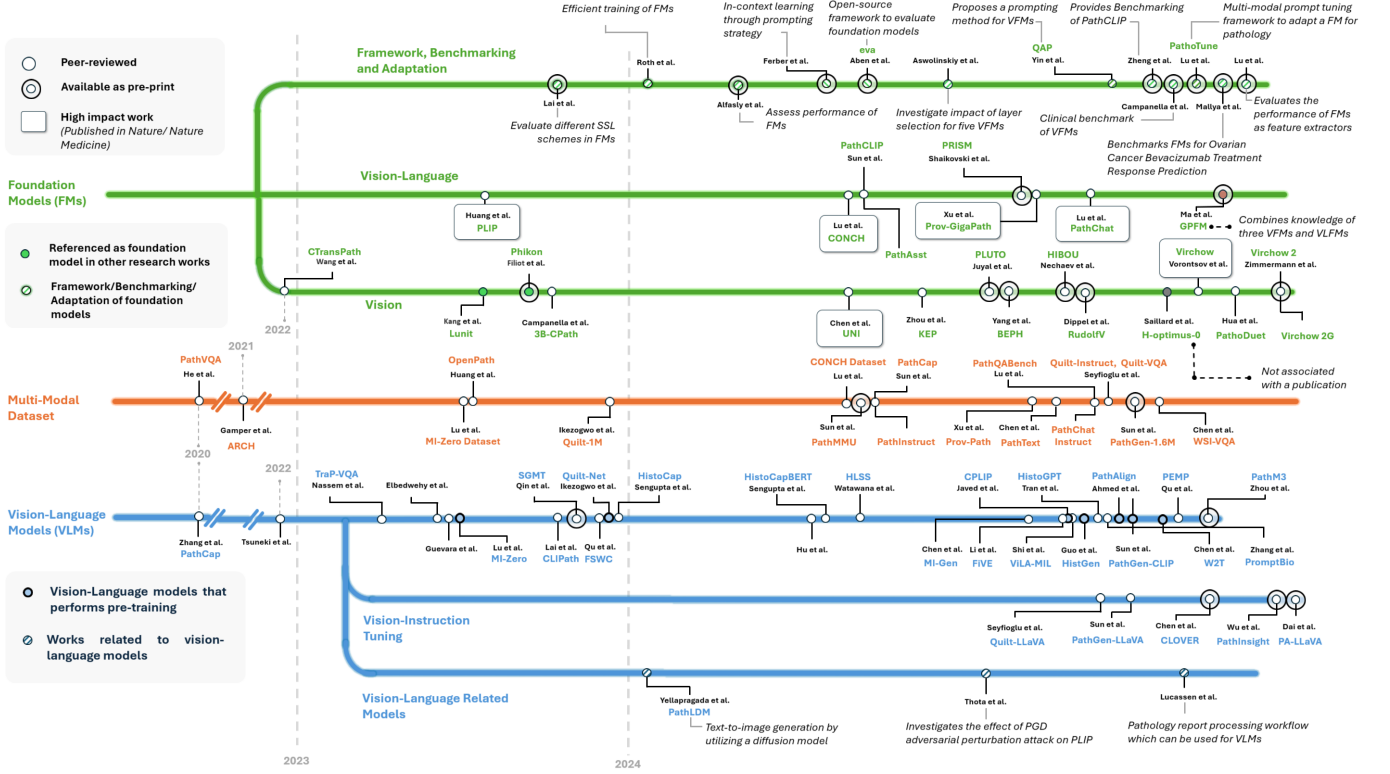


Fig. 3. Visualization of the timeline of recently published work in CPath utilizing FMs and VLMs as well as multi-modal datasets. To maintain transparency, we clearly annotate research articles that have been peer-reviewed and articles that are available as pre-prints. Furthermore, high-impact pioneering research works published in prominent journals are highlighted. For pre-prints if there are multiple versions, the latest version and the corresponding date are used.

ble II, Table IV, Table V, Table VIII) so it is easier for readers to follow.

- 4) Annotated timeline of the surveyed articles (Fig. 3) which provides a clear idea of the evolution of the FMs and VLMs in CPath. In addition, a project page is available (<https://cpath-fms-vlms.github.io/survey/>) with additional information about the surveyed articles.

The rest of the article is organized as follows: in section II existing multi-modal datasets are listed along with details about their source, pre-processing techniques, etc. Section III outlines existing FMs in CPath and descriptions for the vision and vision-language pre-training schemes for those FMs are provided. In section IV an extensive list of VLMs in CPath is presented along with details of their architectures, utilized datasets and contributions. Finally, section V concludes the paper.

II. MULTI-MODAL DATASETS IN PATHOLOGY

In this section, a comprehensive summary of the existing multi-modal datasets available in CPath is provided. The modalities taken into account are vision and language. All key information regarding each dataset is summarized in Table II.

To have a comprehensive understanding of the existing multi-modal datasets for pathology, three different components need to be considered as shown in Fig. 4.

A. Type of Datasets:

The first component is the type of data which can be broadly classified into 5 categories. Prov-Path [38] fall into

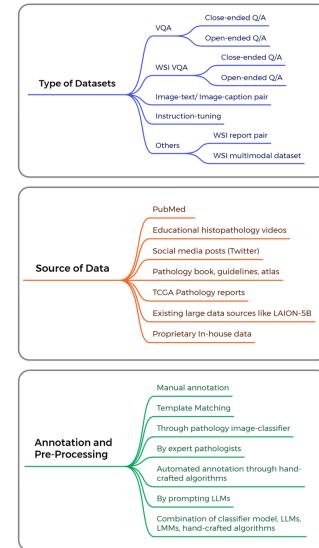


Fig. 4. Different components of multi-modal datasets in computational pathology: Type of datasets, sources of data, annotation and pre-processing

the last category which is dissimilar to the rest of the datasets. The dataset for Prov-Path utilizes WSI and the corresponding reports along with histopathology findings, cancer staging, genomics mutation profiles, etc. collected by Providence Health System (PHS).

The rest of the datasets can be sectioned into the re-

TABLE II
SUMMARY OF MULTI-MODAL DATASETS IN PATHOLOGY

Dataset	Type of Data	Size	Image and Text Source	Method of Generation/Procurement	Other Utilized Dataset/Models for Generation/Procurement	Dataset Used By	Variation/Subset/Extension	Availability (Linked)
WSI-VQA [49]	WSI and Q/A pairs	977 WSIs 8,672 question-answer pairs (slide-level) with average 8.9 Q/A pairs per WSI	WSI and pathology report from TCGA-BRCA	Prompting LLMs and template matching heuristics	Model/Framework: GPT-4 [50]	Wsi2Text Transformer (W2T) [49]	4535 close-ended VQA subset and 4137 open-ended VQA subset	✓
PathGen-1.6M [51]	Image-caption pairs	1.6 million	WSI and pathology report from TCGA	Multi-agent collaboration and caption generation with large multimodal models (LMMs)	Dataset: PathCap [40], Quilt-1M [52], OpenPath [42] Model/Framework: LLaVA-v1.5 [53], Vicuna [54] OpenCLIP [55], GPT-4 [50]	PathGen-CLIP [51], PathGen-LLaVA [51]	200K instruction-tuning data (Extension)	✓
Quilt-Instruct [56]	Instruction-tuning question-answer pairs	107,131 histopathology-specific Q/A pairs	Over 1,000 hours of 4,149 educational histopathology videos from YouTube	Prompting GPT-4, hand-crafted algorithms for extraction of video frames and spatial annotation	Dataset: Quilt-1M [52] Model/Framework: GPT-4 [50]	Quilt-LLaVA [56]	Quilt-VQA with 985 images 1,283 Q/A pairs where 940 are open-set and 343 closed-set	✓
PathQABench [37]	ROI-annotated WSI and Q/A	48 H&E WSIs (25 WSIs from PathQABench-Private 23 WSIs from PathQABench-Public) + 48 close-ended Q/A 115 open-ended Q/A	PathQABench-Private from private in-house cases PathQABench-Public from TCGA cases	Expert-pathologists curated and annotated	—	PathChat [37]	(Subsets) PathQABench-Public and PathQABench-Private PathChatInstruct 456,916 instruction-tuning dataset (Extension)	✓
PathText [57]	WSI and question-text pairs	1,041 WSI 9,009 WSI-text pairs	WSI and pathology report from TCGA-BRCA	Prompting LLMs, OCR, manual annotation, classifier	—	MI-Gen [57]	—	✓
Prov-Path [38]	WSI and reports pairs	17,383 WSI-reports pairs	Proprietary dataset from Providence Health System (PHS)	K-means to generate four representative reports which are used to prompt GPT 3.5 to clean rest of the reports	Model/Framework: GPT-3.5	Prov-GigaPath [38]	—	✓
PathCap [40]	Image-caption pairs	207K	PubMed, internal pathology guidelines books, annotation by expert cytologists	Parsing from PubMed, image processing with YOLOv7, ConvNeXt, PLIP, caption refinement and text processing with ChatGPT	Dataset: PubMed Model/Framework: YOLOv7 [58], ConvNeXt [59] ChatGPT [60], PLIP [42]	PathAsst [40]	PathInstruct 180K pathology multimodal instruction-following samples (Extension)	✓
PathMMU [61]	Image and Q/A pairs	24,067 pathology images 33,428 Q/A	PubMed, pathology atlas, educational videos, pathologist-shared images with explanations on Twitter	Prompting GPT-4, heuristics, annotation by seven pathologists	Dataset: Quilt-1M [52], OpenPath [42] Model/Framework: GPT-4 [50], YOLOv6 [62]	—	PubMed, SocialPath EduContent, Atlas, PathCLS (Subsets)	✓
Dataset from CONCH [41]	Image-caption pairs	1,786,362 image-caption pairs	PubMed, publicly available research articles, internal data from Mass General Brigham institution	Hand-crafted workflow with YOLOv5, CLIP, BioGPT	Model/Framework: YOLOv5 [63], CLIP BioGPT [64]	CONCH [41]	PMC-Path (data from PubMed) EDU (data extracted from educational notes)	✓
QUILT [52]	Image-text pairs	437,878 images aligned with 802,144 text pairs	1,087 hours of 4,504 narrative educational histopathology videos from YouTube	Prompting LLMs, hand-crafted algorithms, human knowledge databases (UMLS), automatic speech recognition	Dataset: OpenPath [42], PubMed, LAION-5B [65] (For Quilt-1M) Model/Framework: Whisper [66], GPT-3.5, inaSpeechSegmenter [67], langdetect [68]	Quilt-Net [52]	Quilt-1M with 1 million image-text pair with additional data from LAION, Twitter, and PubMed (Extension)	✓
OpenPath [42]	Image-text pairs	208,414 image-text pairs	116,504 image-text pairs from Twitter posts, 59,869 image-text pairs from replies, 32,041 image-text pairs from LAION-5B	Pathology image classifier to exclude non-pathology images, CLIP image embeddings with cosine similarity to create PathLAION, other hand-crafted heuristics	Dataset: LAION-5B [65] Model/Framework: CLIP [45], langdetect [68]	PLIP [42]	PathLAION 32,041 pathology images from the LAION-5B dataset (Subset)	✓
Dataset from MI-Zero [69]	Image-caption pairs	33,480 image-caption pairs	Publicly available educational resources combined with ARCH	Hand-crafted algorithms to filter out non-pathology images	Dataset: ARCH [70]	MI-Zero [69]	—	✓
ARCH [70]	Image-caption pairs	11,816 image-caption pairs	PubMed and pathology textbooks	Hand-crafted algorithms with tools like PubMed Parser, Pdffigures 2.0	Model/Framework: PubMed Parser [71] Pdffigures 2.0 [72]	—	—	✓
PathVQA [73]	Image and Q/A pairs	4,998 images 32,799 Q/A pairs	Pathology textbooks, Pathology Education Informational Resource (PEIR) digital library	Hand-crafted algorithms with tools like PyPDF2, PDFMiner, Stanford CoreNLP toolkit	Model/Framework: PyPDF2, PDFMiner Stanford CoreNLP toolkit [74]	—	16,465 open-ended Q/A subset, 16,334 close-ended Q/A subset	✓

Availability: GitHub repositories (except for ARCH [70] and PathVQA [73]; direct dataset source is linked for these two papers) with the associated paper are linked if they are open-sourced and accessible. Some repositories only provide data generation and processing code (if the data is proprietary or requires an API) and some provide direct data sources through platforms such as Hugging Face Hub, Zenodo.
Other Utilized Dataset/Models: Dataset/Models/Framework used only in the data generation/processing part is mentioned. The downstream task datasets are not mentioned for this reason.

maining four categories. The image-caption/image-text pair category (dataset from CONCH [41], PathGen-1.5M [51], Quilt-1M [52], PathCap [40], OpenPath [42], dataset from MI-Zero [69], ARCH [70]) involves a low or medium-quality image and an associated piece of text for that image. This text can be a short caption with a description of the image or a more elaborate description. ARCH is the earliest dataset in this category that utilized PubMed and pathology textbooks to extract the texts. PathGen-1.5M is the latest dataset in this category, but unlike other datasets in this category, the images are patches extracted from WSIs.

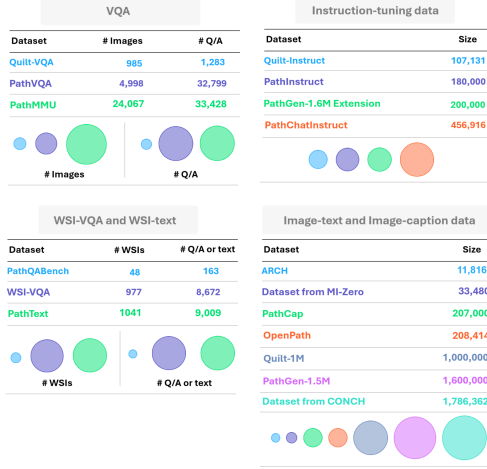


Fig. 5. Comparison between the size of different multi-modal datasets. The size of the bubbles indicates the size of the data set (For visual clarity, the scale used for bubble size is the same within a specific group, but differs between groups).

This is in contrast to other datasets in this category like OpenPath [42] which is constructed with Twitter posts and replies and Quilt-1M [52] which is constructed with frames extracted from educational pathology videos. However, the curation and annotation process of this category is much easier as it can be automated with hand-crafted algorithms and heuristics. However, it comes with an inevitable noisy data as due to the automated process a lot of artifacts can be present in the data.

The WSI VQA/text category (WSI-VQA [49], PathQABench [37], PathText [57]) contains question and answer pairs or texts associated with WSIs. The most common data source is the cancer genome atlas (TCGA) [20] which contains a large repository of WSI and patient report pairs. The VQA part can be of two types, close-ended question-answer pair and open-ended question-answer pair. Close-ended question-answer pairs are of a multiple-choice type or short-answer type which have pre-defined answers. On the other hand, open-ended question-answer pairs contain answers that are in natural language form. Among the datasets in this category, PathQABench is unique as it contains region of interest (ROI) annotation of WSIs performed by expert pathologists. It has two subsets as PathQABench-Public and PathQABench-Private. The former is publicly available as it was constructed with TCGA WSIs and reports, and the latter was constructed with in-house data.



Fig. 6. Subsets of the **Quilt-1M** dataset and the corresponding number of image-text pair for each subset.

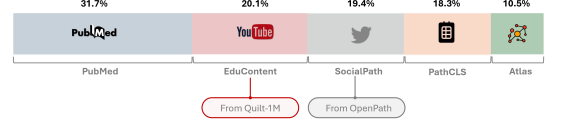


Fig. 7. Subsets of the **PathMMU** dataset and proportion for each subset. The EduContent and SocialPath subset is sourced from Quilt-1M and OpenPath dataset.

The next category, which is VQA (PathMMU [61], Quilt-VQA [56], PathVQA [73]) is similar to the previous category as it also contains close-ended and open-ended question-answer pairs, but the associated images are not WSIs but rather low and medium-quality images. Among these datasets, PathVQA is the first research to curate a pathology-specific VQA dataset. PathMMU is the latest and largest dataset in this category and it also provides explainability annotations with each answer. Another category, which is the instruction-tuning dataset (Quilt-Instruct [56], PathInstruct [51], PathChatInstruct [37], extension of PathGen-1.6M [51]) is a unique kind of dataset, as this type of dataset is used to provide conversational ability to an existing multimodal model. The common workflow is that the instruction-tuning dataset is applied in the last phase to fine-tune an already trained VLFM or VLM. All of these datasets were created following the strategy mentioned in LLaVA [53] or LLaVA-1.5 [75]. More details about the instruction-tuning phase are provided in section III-C and section IV-C.

A comparison of dataset sizes is shown in Fig. 5.

B. Source of Data:

The second component to consider is the source of data which largely dictates the third component, the annotation and pre-processing. PubMed is a common data source containing pathology images and captions/text. However, the quality of the data is not as high as that of the TCGA repository that contains WSIs and corresponding pathological reports. Other high-quality data sources that contain WSIs and pathology reports are in-house proprietary datasets (PathQABench-Private, Prov-Path). A unique data source, OpenPath, contains pathology images and texts from Twitter posts and replies associated with a large pathology community.

This data set was supplemented by pathology-specific data from the large-scale artificial intelligence open network (LAION) data repository [65]. Pathology textbooks and Atlas are also large knowledge sources that can be used to extract image caption/text pairs. In a couple of recent research [52], [56], educational histopathology videos on YouTube are being used as the source of pathology image and text pair. However, curation of this kind of dataset requires a series of hand-crafted algorithms and many external tools. Based on the above

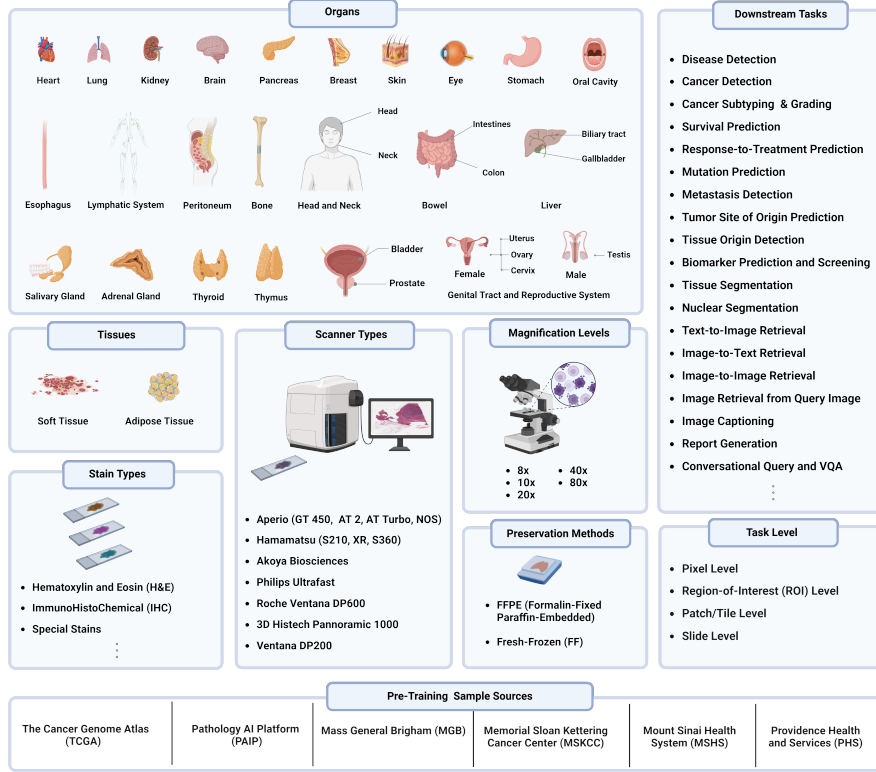


Fig. 8. A high-level visualization of different factors of variability in terms of organs, stain types, scanner types, magnification levels, preservation methods, downstream tasks, task levels, pre-training tissue sample sources, etc. in foundation models. The research that puts the most emphasis on ensuring variability are RudolfV [26] and PLUTO [29]. Among the tissue sample sources for pre-training, TCGA and PAIP are publicly accessible and the rest are proprietary.

discussion, it is apparent that there is a trade-off between the quality and volume of the data.

Another key point is that most of these datasets contain other datasets as one of the subsets. An example of that is Quilt-1M which contains OpenPath, PubMed and LAION as subsets in addition to the proposed Quilt dataset. A visualization of Quilt-1M and its subsets is provided in Fig. 6. Another such example is the PathMMU dataset (shown in Fig. 7) which contains 5 different subsets, PubMed, SocialPath, EduContent, Atlas and PathCLS each containing data from different sources.

C. Annotation and Pre-Processing:

The third component is the annotation and pre-processing steps of data curation and generation. Among the surveyed articles, all employ a series of steps depending on the type of dataset and the pre-processing pipeline is unique for every article. However, some specific steps are similar if the data source is the same. For example, all articles that utilize PubMed as a data source use some kind of parsing process [71] to parse and extract figures and texts. In addition, they employ light-weight classifiers and object detection architectures (YOLOv5 [63], YOLOv6 [62], YOLOv7 [58]) to distinguish between pathology and non-pathology images, detect and separate subfigures, etc. Another common approach is to prompt LLMs to format and refine captions/text or structure extracted information according to a pre-defined template. These LLMs include generalized LLMs like GPT-4, GPT-3.5, ChatGPT and

also specialized LLMs like BioGPT. Another widely used strategy is using a trained CLIP-based model and using cosine similarity as a metric to classify pathology and non-pathology images.

Apart from the approaches mentioned above, there are a lot of other hand-crafted algorithms, heuristics and tools which are summarized in Table II.

III. FOUNDATION MODEL

In this section, an overview of existing FMs in CPath is provided. First, the characteristics of FMs (section III-A) are provided to remove any ambiguity for the later sections. Next, pre-training workflow and typical pre-training schemes (section III-B) are mentioned along with the instruction-tuning phase (section III-C) which is becoming a widely adopted technique to provide FMs with conversational ability. Next, the downstream tasks and the associated downstream datasets (section III-D) for the FMs are outlined.

A. Characteristics of FMs

A model can be classified as FM if it holds the following characteristics :

- 1) The first characteristic that is common to all FMs is the SSPT. The data used in the pre-training phase do not have any explicit label or annotation.
- 2) The training goal of FMs is not to solve any specific task but rather to learn a general and rich representation

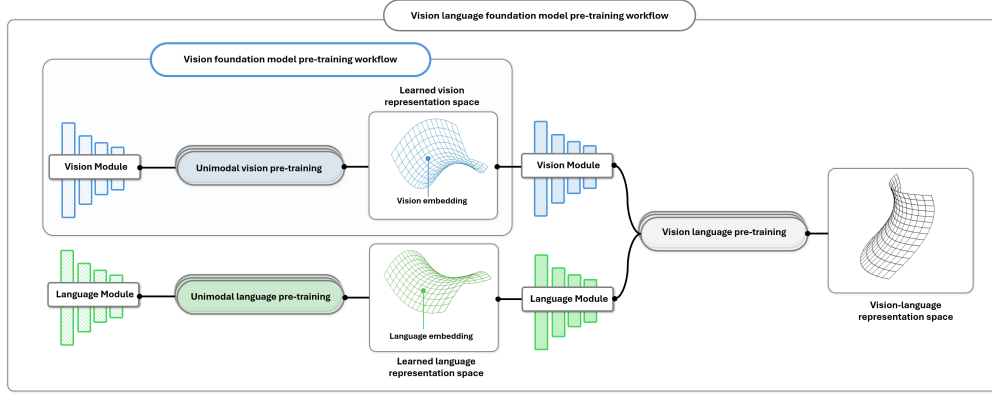


Fig. 9. Typical pre-training workflow in FMs. In general it starts with a vision module and a language module with randomly initialized weights or pre-set weights. VFMs only go through unimodal vision pre-training to learn a vision representation space. On the other hand, VLFMs can optionally go through unimodal pre-training for their vision and language modules.

space. For VFMs, it is a vision representation space and for VLFMs it is a vision-language representation space. The training of FMs is termed as “pre-training” as in later stages further training is required to optimize for a specific task.

- 3) In CPath, FMs are trained using large and diverse datasets that encompass tissue samples from different organs and anatomic sites. In addition, some research [26], [29] put effort into capturing diversity in terms of scanner types, magnification levels, stain types, preservation methods, etc. The idea is to capture the representation of a wide range of tissue and disease types. In Fig. 8 a high-level visualization is provided highlighting different aspects of FMs.
- 4) Another characteristic is the size of models that typically have parameters on the scale of millions. A huge amount of computing resources is put into training these models involving multiple GPUs.

As shown in Fig. 3, the FMs are sectioned into three separate categories. One category encompasses VFMs [22]–[35] in CPath, the second category encompasses VLFMs [36]–[42] and the last category utilizes these FMs by providing a benchmark, framework or adapting existing FMs [76]–[87].

B. Pre-training Workflow and Strategies

The typical pre-training workflow of FMs is shown in Fig. 9 which provides a high-level visualization of different phases in the workflow.

In this single diagram, both pre-training strategy for VFM and VLFM is shown. For VFMs, a vision module with some initial weight is leveraged in pre-training. The term “vision module” is used to generally represent a wide range of vision architectures and also modified versions of these architectures with additional layers. The most common architecture is variants of vision image transformers (ViTs) [88] which includes ViT-S, ViT-B, ViT-L, ViT-G and ViT-H. Though there are specialized architectures proposed in BEPH [28] and Prov-GigaPath [38] which uses BEiTv2 [89] and GigaPath architecture, respectively. Note that, some models initialize the architectures with ImageNet [90] weights to get an initial

vision representation space which can be transformed through pre-training. In Table III, a summary of pre-training strategies in different phases is outlined.

TABLE III
DIFFERENT PRE-TRAINING PHASES AND CORRESPONDING SSPT STRATEGIES

Pre-training phase	Strategy	
Unimodal vision pre-training	Self-Distillation	DINO [91], DINOv2 [92]
	Contrastive Learning	MoCov2 [93], MoCov3 [94]
	Masked Image Modeling (MIM)	MAE [95], iBOT (MIM+Self distillation) [96]
Unimodal language pre-training	No Specific Strategy	
Vision-language pre-training	CLIP [45], CoCa [97]	

The term “unimodal” is used to signify the pre-training phase utilizing a single modality out of vision and language. This is inherently different from vision-language pre-training strategies which involve both vision and language modalities to learn a joint vision-language representation space. In the unimodal vision pre-training phase there are three strategies commonly used in CPath which are self-distillation, contrastive learning and masked image modeling (MIM) approach. Each approach has its own advantages and disadvantages.

The work done in Lunit [34] benchmarks DINO [91], MoCov2 [93], SwaV [100], Barlow Twins [101] but concludes there is no clear best SSPT scheme. However, the authors conclusively prove that SSPT always outperforms ImageNet initialization.

1) *Unimodal Vision Pre-training*: The self-distillation with no label approach uses a student-teacher network to learn a rich vision representation space as shown in Fig. 10. From a single image patch, two different views are generated by applying an augmentation sampled from a set of possible augmentations (color jittering, Gaussian blur, polarization, etc). The generated output of both the networks is utilized to compute a cross-entropy loss which is then used to update the parameters of the student network. The parameter of the teacher network is then updated through an exponential

TABLE IV
SUMMARY OF VISION PRE-TRAINING STRATEGY AND VISION PRE-TRAINING DATASET OF FOUNDATION MODELS IN PATHOLOGY

Model	Vision Pre-Training Strategy			Vision Pre-Training Dataset				Type of Foundation Model	Availability (Linked)
	Category	Approach	Architecture	Source	Size	Stain	Additional Information		
GPfM [36]	MIM + Self-Distillation+ (Expert Knowledge Distillation)	Custom	Custom architecture that uses other FMs including UNI, Phikon, CONCH	33 public datasets including TCGA, GTExPortal PAIP, CPTAC, etc	Slides: 86,104 Tiles: 190,000,000	—	47 data sources 34 major tissue types	Combines Knowledge of VFMs and VLFMs	✓
Virchow 2 [22]	Self-Distillation	DINOv2	ViT-H	Memorial Sloan Kettering Cancer Center (MSKCC) + Institutions worldwide	Slides: 3,134,922 Tiles: —	H&E IHC	225,401 patients 493,332 cases 871,025 specimens	Vision	✓
Virchow 2G			ViT-G						
PathoDuet [23]	Contrastive Learning	MoCov3	ViT-B	TCGA	Slides: 11,000 Tiles: 13,166,437	H&E	—	Vision	✓
Virchow [24]	Self-Distillation	DINOv2	ViT-H	Memorial Sloan Kettering Cancer Center (MSKCC)	Slides: 1,488,550 Tiles: 2 billion	H&E	17 organs 119,629 patients 208,815 cases 392,268 specimens	Vision	✓
RudolfV [26]	Self-Distillation	DINOv2	ViT-L	108,433 slides from 15 labs across the EU and US + 26,565 slides from TCGA	Slides: 133,998 Tiles: 1.2 billion	H&E (68%) + IHC (15%) + other (17%)	14 organs 15 lab 58 tissue types 129 stains 6 scanner types FFPE and FF tissue	Vision	—
Hibou [27]	Self-Distillation	DINOv2	ViT-B (for Hibou-B) ViT-L (for Hibou-L)	Proprietary Data	Slides: 936,441 H&E +202,464 non-H&E + 2,676 cytology slides Tiles: 1.2 billion patches for Hibou-L, 512 million patches for Hibou-B	H&E + non H&E	306,400 cases	Vision	✓
BEPH [28]	MIM	—	BEITv2 [89] with VQ-KD autoencoder and ViT-B encoder	TCGA	Slides: 11,760 Tiles: 11,774,353	H&E	32 cancer types	Vision	✓
PLUTO [29]	Self-Distillation+MIM	DINOv2 variation + MAE	ViT-S variant FlexiViT-S [98]	TCGA + Proprietary data from PathAI	Slides: 195 million Tiles: 158,000	H&E + IHC + Other stains	More than 30 diseases More than 12 scanners More than 100 stain types More than 4M pathologist pixel-level annotation	Vision	—
UNI [31]	Self-Distillation	DINOv2 (also MoCov3 for comparison)	ViT-L	Proprietary Data from Massachusetts General Hospital (MGH), Brigham and Women's Hospital (BWH), Genotype-Tissue Expression (GTEx) consortium	Slides: 100,426 Tiles: over 100 million	H&E	20 major tissue types	Vision	✓
3B-CPath [32]	MIM and Self-Distillation	MAE, DINO	ViT-S, ViT-L	Mount Sinai Health System (MSHS)	Slides: 423,600 Tiles: 3.25 billion	H&E	3 anatomic site 2 institutions	Vision	✓
Phikon [33]	MIM+Self-Distillation	iBOT	ViT-S, ViT-B, ViT-L	TCGA (Three variants TCGA-COAD, PanCancer4M, PanCancer40M)	Slides: 6,093 Tiles: 43,374,634 (For PanCancer40M)	H&E	16 cancer types 13 anatomic sites 5,558 patients (For PanCancer40M)	Vision	✓
CTransPath [35]	Contrastive Learning	MoCov3 variation (SRCL: semantically relevant contrastive learning)	Swin Transformer	TCGA + PAIP	Slides: 32,220 Tiles: 15.6 million	H&E	32 cancer types 25 anatomic sites	Vision	✓
Prov-GigaPath [38]	MIM and Self-Distillation	MAE, DINOv2	GigaPath [38] (constructed with ViT and LongNet [99])	Providence Health System (PHS)	Slides: 171,189 Tiles: 1.3 billion	H&E, IHC	30,000 patients 28 cancer centers 31 major tissue types	Vision Language	✓
CONCH [41]	MIM + Self-Distillation	iBOT	ViT-B backbone in image encoder	In-house dataset	Slides: 21,442 Tiles: 1.2 million	H&E, IHC, Masson's trichrome, Congo red	350 cancer subtypes	Vision Language	✓

moving average (EMA) of the student network parameters. Among the surveyed articles Virchow2 [22], Virchow [24], RudolfV [26], Hibou [27] and UNI [31] use DINOv2 [92] as the self-distillation approach. PLUTO [29] takes a unique approach by integrating MAE and a Fourier loss term to get a custom variation of DINOv2.

The second popular SSPT approach is the MIM (visualized in Fig. 11) which has variants like MAE [95] and iBOT [96] used in FMs. In the MAE approach, randomly selected high portions of the image are masked out and the patches that are not masked out are passed through an encoder which generates latent representations of those patches.

Then those representations are passed through a decoder along tokens of masked out regions to reconstruct the image

and reconstruction loss is used to train the model. The iBOT approach also uses MIM but adds self-distillation technique by leveraging a student-teacher network. The teacher network works as an online tokenizer and the student network learns to predict masked patches with the help of distilled knowledge of the teacher network.

Among the surveyed articles 3B-CPath [32] and Prov-GigaPath [38] use MAE but in conjunction with DINO and DINOv2, respectively. Research works utilizing iBOT approach include Phikon [33] and CONCH [41].

Another SSPT approach that is comparatively less popular in FMs for CPath is the contrastive learning framework proposed in MoCo [105] (visualization in Fig. 12). Over the years variations of the proposed approach in MoCo in terms

TABLE V
SUMMARY OF VISION-LANGUAGE PRE-TRAINING AND INSTRUCTION TUNING PHASE OF FOUNDATION MODELS IN PATHOLOGY

Model	Vision Language Modules			Vision-Language Pre-Training Phase		Instruction Tuning Phase	
	Vision Module	Language Module	Additional Layer/Module	Architecture / Framework	Pre-Training Process	Instruction Tuning	Process
PathChat [37]	UNI [31] as vision encoder backbone	Pre-trained Llama 2 [102] LLM which is a decoder-only transformer-based auto-regressive model	A multimodal projector module to connect the outputs of the vision module to language module by projecting the visual tokens to the same dimension as the LLM's embedding space for text tokens	CoCa	Vision-language pre-training according to CoCa framework with CONCH dataset	✓	LLaVA-1.5 [75] training approach First phase: Only the parameters of multi-modal projector is updated Second phase: Fine-tuned with instruction-following data
PRISM [39]	Virchow as tile encoder, Perceiver [103] as slide-encoder	BioGPT first 12 layers	BioGPT last 12 layers as vision-language decoder	CoCa	Trained using contrastive loss and generative/captioning loss	✗	—
PathCLIP and PathAsst [40]	Image encoder with ViT-B	Text transformer as the text encoder with modifications mentioned in [104]	Fully-connected layer after vision encoder to map the image embedding space to the corresponding language embedding	CLIP	Fine-tuning of CLIP model through contrastive learning using PathCap dataset	✓	First phase: Detailed description-based part is used to train the fully-connected layer connected to the vision encoder. Second phase: fine-tuned with instruction-following data via next word prediction
CONCH [41]	An image encoder with ViT-B backbone with 12 transformer layers, 12 attention heads followed by two attentional pooler modules	A GPT-style text encoder with 12 transformer layers	A GPT-style multimodal decoder with 12 transformer layers	CoCa	Visual-language pre-training with image-text contrastive loss and the captioning loss according to CoCa framework	✗	—
PLIP [42]	An image encoder with ViT-B	A text transformer as the text encoder with modifications mentioned in [104]	—	CLIP	Fine-tuning of CLIP model through contrastive learning using OpenPath dataset	✗	—

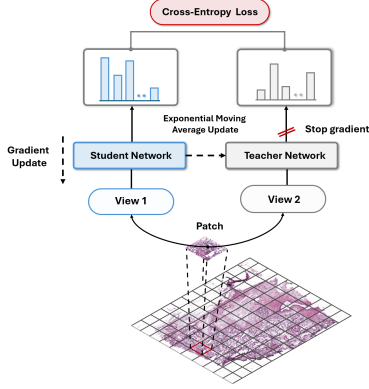


Fig. 10. Visualization of the self-distillation approach for unimodal vision pre-training scheme.

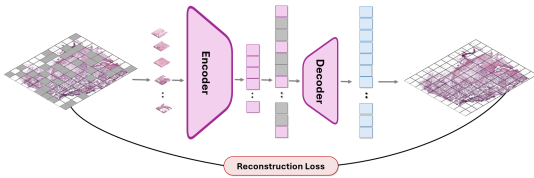


Fig. 11. Visualization of the masked image modeling approach for unimodal vision pre-training scheme.

of architectural change and training blueprint have been done and MoCov2 [93] and MoCov3 [94] are the results of that.

Like the self-distillation approach, MoCo also utilizes two models; one is an encoder (with query patch as input) and the second one is a special momentum encoder (with key patches as input). The embeddings generated through the encoder and the momentum encoder are used to compute a similarity

score which in turn is used for contrastive loss computation. The computed loss is used in backpropagation to update the parameters of the encoder. The parameter of the momentum encoder is updated through a momentum-based update rule that utilizes the parameters of the encoder. Another innovation

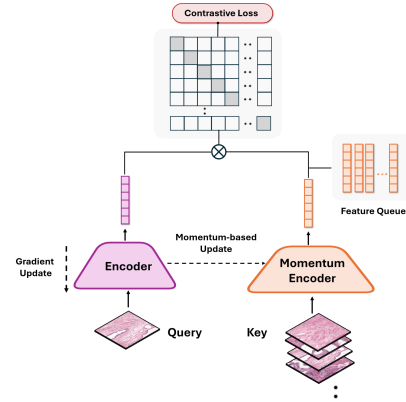


Fig. 12. Visualization of the MoCo approach for unimodal vision pre-training scheme.

of MoCo was introducing a feature queue which ensures a large set of negative samples without holding the entire dataset in memory. This also ensures the negative samples do not go stale over the training period and the model sees a diverse set of negative samples to learn a better vision representation. Among the surveyed articles PathoDuet [23] uses MoCov3, UNI [31] uses MoCov3 for comparison and CTransPath [35] performs a unique variation of MoCov3 called semantically relevant contrastive learning (SRCL). GPFM [36] is distinct from other approaches as it includes a novel expert knowledge

distillation in addition to MIM and self-distillation by utilizing existing FMs UNI, Phikon and CONCH.

2) *Unimodal Language Pre-Training*: Most VLFMs do not perform large-scale unimodal language pre-training. Instead, they rely on already pre-trained in-domain (trained with medical corpus) LLMs like BioGPT or other LLMs like Llama 2, GPT-variants, etc. One exception is CONCH which pre-trains the language module with 550,000 surgical pathology reports from Massachusetts General Hospital and over 400,000 select histopathology-relevant PubMed abstracts.

3) *Vision-Language Pre-training*: After unimodal pre-training for the image module and text module, VLFMs might go through vision language SSPT to align or learn a joint vision-language representation space.

The most popular vision-language SSPT approach in CPath is the CLIP approach shown in Fig. 13.

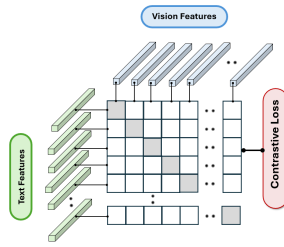


Fig. 13. Visualization of the CLIP approach for the vision-language pre-training scheme.

The inputs to CLIP are a batch of image features encoded by an image encoder and a batch of text features encoded by a text encoder. The model is trained to pull together the corresponding image feature and text feature in the representation space and push apart the rest of the features i.e. utilizing a contrastive objective. In other words, maximizing the similarity (specifically cosine similarity) between the corresponding image and text pair while minimizing the cosine similarity with other non-matching embeddings in the representation space.

The second widely used approach is the contrastive captioner (CoCa) [97] framework shown in Fig. 14. It contains

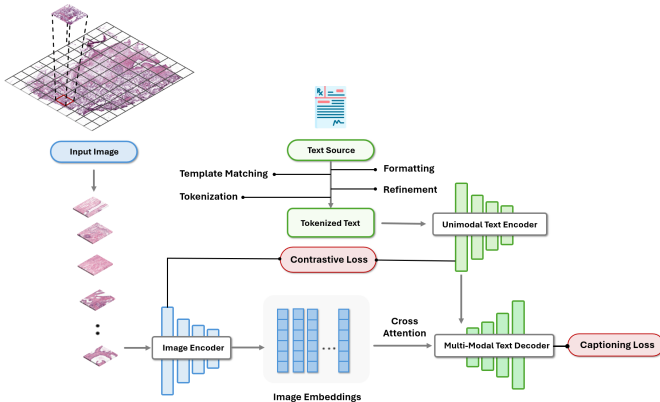


Fig. 14. Visualization of the CoCa approach for the vision-language pre-training scheme.

three different modules; an image encoder, an unimodal text encoder and a multi-modal text decoder. It is trained by

leveraging both captioning loss which follows a generative objective and contrastive loss which follows a contrastive objective. The input image patches are passed through an image encoder to generate image embeddings which is used to provide cross-attention to the multi-modal text decoder. The combination of generative and contrastive objectives forces the model to learn rich vision-language representation space.

Details of vision modules, language modules, additional modules and specifics of the pre-training process of FMs are outlined in Table V.

One recent work KEP [30] proposes an entirely new approach in visual-language SSPT named knowledge enhanced pre-training by utilizing PathKT, a pathology knowledge tree curated by the same research. This is different from the CLIP and CoCa pre-training techniques as it uses a novel knowledge encoder and knowledge distillation technique.

C. Instruction-Tuning Phase

For CPath, the instruction-tuning phase provides the model with conversational ability i.e. a user can prompt the model and the model will respond according to the prompt. Visual-instruction tuning adds the ability to provide an image in addition to natural language user prompts. Among the surveyed papers in FMs, PathChat and PathAsst perform instruction-tuning with self-curated datasets PathChatInstruct and PathInstruct, respectively. Both works adopt the strategy employed by LLaVA and LLaVA-1.5 which are the pioneering work in visual instruction tuning. A summary of the instruction tuning process is provided in Table V. For both PathChat and PathAsst, the instruction tuning phase is subdivided into two phases. For both models in the first phase, the parameters of the vision encoder are frozen and the layer/module connected to the vision encoder (for PathChat it is a multimodal projector, for PathAsst it is fully connected layers) is trained. In the second phase, the model is fine-tuned with instruction-following data. More details about visual instruction tuning and a description of research work exclusively focusing on this aspect in CPath are provided in section IV-C.

D. Downstream Tasks and Datasets

FMs have the ability to adapt to a vast array of tasks by utilizing the representation space learned during SSPT.

Note that, in the pre-training phase FMs were never trained for any of these specific tasks. At the end of the pre-training of FMs, one of the following strategies is adopted to perform a specific task.

- 1) **Linear Probing**: This is a commonly used technique where a linear classifier/regressor is trained on top of the pre-trained model. During the training of the linear layers, the parameters of the pre-trained model are kept frozen. Depending on the specifics of the tasks, the corresponding loss function and update rule are determined. This is a computationally cheap way to adapt to a downstream task as the parameters of the pre-trained model do not need to be updated.

TABLE VI
DIFFERENT TYPES OF DOWNSTREAM TASKS AND CORRESPONDING
RESEARCH WORKS

Downstream tasks	Performed By
Disease/Cancer/Tissue/Tumor/Molecular SubTyping	[42], [41], [39], [38], [23], [31], [28], [26], [30], [35], [29]
Cancer Detection	[22], [42], [39], [23], [32], [28], [24], [35]
Tumor Detection	[42], [40], [31]
Cancer Grading	[41], [31]
Image/Tissue/Tumor/Gland/Nuclei Segmentation	[41], [31], [26], [35], [29]
Survival Prediction	[28]
Text-to-Image Retrieval	[42], [41], [30]
Image-to-Text Retrieval	[41], [30]
Image-to-Image Retrieval	[42], [31], [26], [36]
Image Captioning	[41]
Pattern/Tissue/Image Classification	[41], [40], [31]
Biomarker Prediction/Detection/Screening/Scoring	[39], [31], [32], [26], [24]
Metastasis Detection	[31], [33]
Organ Transplant Assessment	[31]
Mutation Detection/Prediction	[38], [31], [32], [33]
VQA	[40], [37], [36]
Report Generation	[39], [36]
Survival Analysis	[22], [36], [33]
Conversational Agent	[40], [37]

- 2) **KNN Probing:** This is yet another approach to adopt a FM for a specific downstream task by utilizing K-nearest neighbors algorithm. In KNN probing a specific representation from learned representation space (through SSPT) is used to find its nearest neighbors.

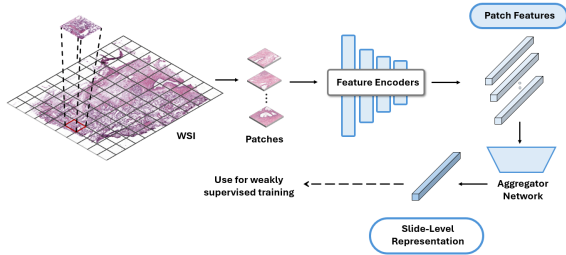


Fig. 15. Aggregate patch-level features through an aggregator network to get a slide-level representation and use it for weakly supervised training.

- 3) **Fine-Tuning:** This is similar to linear probing as a classifier/regressor is added on top of the pre-trained model, but the major difference is the parameter of the pre-trained models is also updated during fine-tuning. Hence, it is computationally much more costly compared to linear probing. This is sometimes also referred to as the supervised training phase. Note that, most of the time annotation is only available on slide-level. Hence, if the slide-level label is utilized it is called weakly supervised training. To attain the slide-level representation from the trained model (which is trained to generate patch-level embeddings), typically a aggregator model is used. A visualization of attaining the slide level representation from the patch embeddings is shown in Fig. 15.

In Table VI, a summary of downstream tasks is provided along with research works performing these tasks. In Table VII a list of downstream datasets utilized by different FMs is provided.

Another aspect to consider is how the performance evalua-

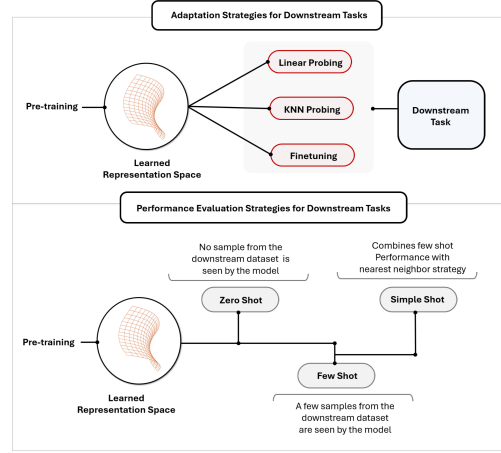


Fig. 16. Adaptation and performance evaluation strategy for downstream tasks.

tion is conducted. Among the surveyed articles, there are three different strategies that are employed.

- 1) **Zero Shot Evaluation:** In zero shot evaluation, the pre-trained model is directly used in a downstream task without probing or fine-tuning the pre-trained model with any samples of the downstream dataset. This provides a direct assessment of learned representation in the pre-training phase i.e. evaluates the quality of the generated embeddings from the pre-trained model. This is the most common approach among the surveyed articles.
- 2) **Few Shot Evaluation:** In few shot evaluation, the pre-trained model sees only a few examples from the downstream task dataset. This is sometimes mentioned as K-shot evaluation where K is the number of data points seen by the model.
- 3) **Simple Shot Evaluation:** Simpleshot [106] is a unique variation of the few shot evaluation methods which is only been explored in UNI. It combines few shot learning with a nearest-neighbor classifier.

A summary visualization for these adaptation and evaluation strategies is given in Fig. 16.

E. Framework, Benchmarking and Adaptation of FMs

There are several research works in CPath that do not directly propose a FM but introduce the framework of FMs, provide benchmarks and comparisons between FMs and adapt the FMs for efficient training.

1) **Frameworks:** eva [83], [107] is a framework for VFMs in CPath which abstracts a lot of complexity of VFMs. In addition, it facilitates the reproducibility of VFMs for fair comparison and provides an interface to evaluate publicly available downstream datasets.

2) **Benchmarking:** Another category is benchmark analysis of FMs [76], [77], [79], [80], [82], [85], [87] in CPath. The work in [76] benchmarks the performance of 6 foundation models (CTransPath, PathoDuet, PLIP, CONCH and UNI) across 5 clinically relevant prediction tasks. The contribution of [77] is benchmarking FMs which include CTransPath, Lunit, Phikon, PLIP, UNI and Virchow for ovarian cancer

TABLE VII
EVALUATION DATASETS AND THE ASSOCIATED MODELS UTILIZING THE DATASET ALONG WITH THE DATA SOURCE

Dataset	Used By	Source
PanNuke	[42], [29]	✓
HEST-1K	[22]	✓
DLBCL-Morph	[22]	✓
TissueNet	[35]	✓
GlaS	[29]	✓
CRAG	[35]	✓
RenalCell	[30]	✓
SkinCancer	[30]	✓
UBC-OCEAN	[36]	✓
Chaoyang	[36]	✓
DigestPath	[42], [41]	✓
WSSS4LUD	[42], [40], [41], [30], [36]	✓
PatchCamelyon (PCam)	[22], [27], [26], [24], [36]	✓
MHIST	[22], [27], [26], [24]	✓
BACH	[28], [31], [30], [36]	✓
SICAP, SICAPv2	[41], [30]	✓
CoNSeP	[24]	✓
KIMIA Path24C	[42]	✓
DHMC	[41], [31]	✓
EBRAINS	[41], [31], [36]	✓
AGGC	[41], [31]	✓
PANDA	[41], [31], [36]	✓
MSK-IMPACT	[39], [24]	✓
SegPath	[31]	✓
BRACS	[31], [36]	✓
UniToPatho	[31], [36], [35]	✓
HunCRC	[31]	✓
BreakHis	[28], [36]	✓
MSI-CRC & MSI-STAD	[27], [26]	✓
TIL-DET	[27], [26]	✓
MIDOG	[22], [24], [35]	✓
CAMELYON16	[28], [23], [31], [36], [33], [35]	✓
CAMELYON17-WILDS	[22], [31], [24], [29], [36], [33]	✓
Kather colon	[42], [28], [23], [29], [30]	
— CRC100K	[40], [41], [31], [27], [26], [36]	✓
— NCT-CRC-HE-100K	[28], [24], [30]	
— NCT-CRC-HE-100K-NONORM	[22], [24]	
LC25000	[40], [28], [30]	
— LC25000Colon	[40], [52]	✓
— LC25000Lung	[40], [52]	
TCGA Uniform	[31]	✓
TCGA CRC-MSI	[31], [36], [24]	✓
TCGA-TILs	[22], [24], [31]	✓
TCGA	[33]	
— TCGA BRCA	[41], [39], [28], [27], [30]	
— TCGA RCC	[41], [28], [27], [23], [30], [35]	✓
— TCGA NSCLC	[41], [39], [28], [27], [23], [29], [30], [35]	

Mentioned data sources are shared through platforms like Zenodo, GitHub, official challenge websites. TCGA dataset needs to be downloaded from the official portal.

bevacizumab treatment response prediction. Another work [79] analyzes the performance of FMs on a large and diverse data set collected from two medical centers. The FMs (CTransPath, UNI, Virchow and Prov-GigaPath) were benchmarked on 3 broad downstream tasks which include disease detection, biomarker prediction and treatment outcome prediction. In [80], the authors benchmark PathCLP [40] on various corrupted images (with 7 corruption types) for 2 downstream datasets. The authors of [82] investigate how layer selection for FMs (CTransPath, Phikon, Lunit + other encoders) affects the downstream task performance. The work done in [85] analyzes different FMs and evaluates their performance on 8 datasets. In [87], the authors evaluate the performance of histopathology-specific SSL methods for 17 unique tissue types and 12 unique cancer types.

3) *Adaptation of FMs*: Another category is the adaptation of existing FMs to carry out tasks such as low-resource fine-tuning [86] and multi-modal prompt-tuning [78]. The work carried out in [86] fine-tunes a FM with a single GPU

and shows that it can outperform SOTA feature extractors. PathoTune [78] adapts a visual or pathology-specific FM to downstream tasks using multi-modal prompts. In [81] the authors propose a task-specific visual prompting approach to tune VFMs. The work done in [84] utilizes in-context learning to learn from prompts without parameter updates. They specifically utilize GPT-4 with vision capability and perform evaluation on 3 downstream datasets.

Other than the surveyed FMs, there are more recent works of FM in CPath like mSTAR [108]. However, as it includes RNA-Seq data in addition to pathology reports it falls outside the scope of this paper. Another foundation model we do not include is H-optimus-0 [25] developed by Bioptimus as it is not associated with a publication.

IV. VISION-LANGUAGE MODELS

In this section, the recent works in CPath with VLMs are outlined. The details about architecture, used datasets and contribution of individual research work are listed in Table VIII.

First, different categorizations of VLMs are provided (section IV-A) to give insight into how VLMs are utilized to solve pathology-specific tasks. Second, the common architectural components in VLMs and adopted strategies are summarized (section IV-B). Then, brief summary of models focusing on visual instruction tuning is provided (section IV-C). Lastly, a brief overview is given for models that do not solve a direct pathology-specific task but perform other types of vision-language tasks (section IV-D).

A. Categorization of VLMs

A categorization of VLMs in CPath can be done based on the reason for using the language modality. Some research works solve tasks like caption generation ([117], [152]–[154], [160]) or VQA ([49], [109]) which necessitates utilization of both vision and language modality because of the nature of tasks. For VQA or caption generation, the generated output from the model needs to be in language form i.e. the model needs to perform a language task. On the other hand, other research works use language modality as a source of semantic information to be injected into information gained from vision modality. This additional semantic information can significantly boost the performance of the model which would not have been possible with a vision-only model. As an example, MI-Zero [69] performs cancer subtyping which is not a language task but utilizes pathology reports curated from the in-house dataset and TCGA as a source of semantic information.

Another categorization can be done by comparing the training approach with FMs. VLFMs are different from VLMs as traditional VLMs focus on solving one or two vision-language tasks like caption generation. However, as FMs become more prevalent recent works are starting to shift towards VLFMs. Recent works (PathGen-CLIP [51], Quilt-Net [52]) take FM-like approach to train their models and adapt them to different downstream tasks. On the other end of the spectrum, there are VLMs that solve only a single task. As shown in Fig. 17

TABLE VIII
SUMMARY OF VISION-LANGUAGE MODELS IN COMPUTATIONAL PATHOLOGY

Model	Architecture and Utilized Models/Frameworks	Dataset	Contribution	Availability
TraP-VQA [109]	<ul style="list-style-type: none"> Question feature extraction with BioELMo [110] and BiLSTM Image feature extraction with ResNet-50 and CNN layers Transformer encoder to fuse question and image feature, transformer decoder to upsample fused features 	PathVQA	<ul style="list-style-type: none"> Performs VQA Provides interpretability in text domain with SHAP [111] Provides interpretability in image domain with Grad-CAM [112] 	—
FSWC [113]	<ul style="list-style-type: none"> CLIP for image and text feature extraction GPT-4 to generate instance-level and slide-level prompt groups which introduce pathological prior knowledge into the model 	<ul style="list-style-type: none"> Camelyon 16 TCGA-Lung In-house cervical cancer dataset 	<ul style="list-style-type: none"> Performs few-shot weakly supervised WSI classification Proposes a two-level (instance-level and slide-level) prompt learning MIL framework named TOP Introduces a prompt guided instance pooling to generate slide-level feature 	✓
ViLA-MIL [114]	<ul style="list-style-type: none"> GPT-3.5 as the frozen LLM which generates visual descriptive text for WSI at 5x and 10x resolution based on class level question prompt ResNet-50 as the image encoder and corresponding CLIP transformer is used as the text encoder Prototype-guided patch decoder which generates slide features and context-guided text decoder which generates text-features 	<ul style="list-style-type: none"> TIHD-RCC (in-house dataset) TCGA-RCC TCGA-Lung 	<ul style="list-style-type: none"> Performs WSI classification with a MIL framework that utilizes information from 5x and 10x. In addition, incorporates information from LLM generated visual descriptive text for both 5x and 10x scale WSIs Introduces a novel prototype-guided patch decoder that progressively aggregates the patch features Introduces a context-guided text decoder to refine the text prompt features by leveraging multi-granular image contexts 	✓
PathM3 [115]	<ul style="list-style-type: none"> ViT-G as the image encoder Query-based transformer to fuse image embeddings of WSIs and corresponding captions Frozen LLM FlanT5 [116] for caption generation 	PatchGastric [117]	<ul style="list-style-type: none"> Performs WSI classification and captioning through a multi-modal, multi-task, multi-instance learning framework Leverages limited WSI captions during training Develops multi-task joint learning inspired from [118] 	—
HLSS [119]	<ul style="list-style-type: none"> ResNet-50 as visual encoder with CLIP pre-training Language encoder from CLIP A positive pairing module (PPM) which consists of three parallel reshape layer followed by MLP A cross-modal alignment (CAM) module which computes cosine similarity 	<ul style="list-style-type: none"> OpenSRH [120] TCGA 	<ul style="list-style-type: none"> Performs hierarchical (patient-slide-patch hierarchy) text-to-vision alignment for SSL Proposes a positive pairing module (PPM) and a cross-modal alignment module (CAM) 	✓
FIVE [121]	<ul style="list-style-type: none"> ResNet as image encoder following [122] Pre-trained BioClinicalBERT [123] as text encoder and utilizing LoRA [124] for fine-tuning GPT-4 to generate fine-grained pathological descriptions based on raw pathology reports and expert inquiries An instance aggregator module consisting of a self-attention module and a cross-attention module that fuses image instance embeddings and prompt embeddings to create bag-level feature 	<ul style="list-style-type: none"> Camelyon 16 TCGA-Lung 	<ul style="list-style-type: none"> Incorporates a patch-sampling strategy for optimize training efficiency of the model Proposes a task-specific fine-grained semantics (TFS) module Performs zero shot histological subtype classification, few shot classification and supervised classification with pre-training 	✓
CPLIP [125]	<ul style="list-style-type: none"> MI-Zero [69] to identity-related prompts based on an image by utilizing similarity metric GPT-3 to categorize and transform prompts into five variations PILP to match the transformed prompts with corresponding images from OpenPath 	<ul style="list-style-type: none"> CRC100K WSSS4LUAD PanNuke DigestPath SICAP Camelyon 16 TCGA-BRCA TCGA-RCC TCGA-NSCLC 	<ul style="list-style-type: none"> Creates a pathology-specific dictionary using a range of publicly available online glossaries Introduces a many-to-many contrastive learning instead of traditional one-to-one contrastive learning 	✓
HistGen [126]	<ul style="list-style-type: none"> GPT-4 to clean and summarize reports curated from TCGA A ViT-L model is pre-trained with 200 million patches by utilizing DINOv2 and used as feature extractor 	<ul style="list-style-type: none"> UBC-OCEAN [127], [128] TUPAC16 [129] Camelyon 16 and 17 TCGA-BRCA TCGA-STAD TCGA-KIRC TCGA-KIRP TCGA-LUAD TCGA-COADREAD 	<ul style="list-style-type: none"> Performs WSI report generation, cancer subtyping and survival analysis Develops a local-global hierarchical encoder module to capture features at different levels (region-to-slide) Develops a cross-modal context-aware learning module to align and ensure interaction between different modalities 	✓
CLIPath [130]	<ul style="list-style-type: none"> ResNet-50 as the vision encoder in CLIP 4 fully-connected layer after the vision encoder Transformer as the text encoder in CLIP 	<ul style="list-style-type: none"> PatchCamelyon (PCam) MHIST 	<ul style="list-style-type: none"> Develops residual feature connection (RFC) to fine-tune CLIP with a small amount of trainable parameters and this also fuses the existing knowledge from pre-trained CLIP and the newly learned knowledge related to pathology-specific tasks 	—
MI-Zero [69]	<ul style="list-style-type: none"> HistPathGPT: Unimodal pre-training of GPT-style transformer (same architecture as GPT 2-medium [104]) which is used as text encoder. Additionally, BioClinicalBERT [131] and PubMedBERT [132] are considered as text encoders. Existing encoders like CTransPath [35] (which is based on Swin Transformer [133]) or ViT-S (ImageNet initialization or pre-trained with MoCov3) 	<ul style="list-style-type: none"> 3 WSI datasets from Brigham and Women's Hospital (in-house dataset) named Independent BRCA, Independent NSCLC, Independent RCC TCGA-BRCA TCGA-NSCLC TCGA-RCC 	<ul style="list-style-type: none"> Performs cancer subtyping with a VLM Develops a custom pathology domain-specific pre-trained text encoder called HistPathGPT Introduces 33,480 image-caption pair dataset 	✓
HistoGPT [134]	<ul style="list-style-type: none"> The vision module is based on CTransPath BioGPT as the language module Image features sampled (with Perceiver Resampler [103]) from the vision modules are integrated into the language module via interleaved gated cross-attention (XATTN) blocks [135] 	<ul style="list-style-type: none"> In-house dataset with 2 cohorts. Munich cohort with 1 6,000 histology samples and Münster cohort with 1,300 histology samples with all samples stained with H&E 	<ul style="list-style-type: none"> Performs histopathology report generation that provides a description of WSIs with high fidelity Provides interpretability map which shows which word in the generated report corresponds to which region in a WSI 	✓

Model	Architecture and Utilized Models/Frameworks	Dataset	Contribution	Availability
PathAlign [136]	<ul style="list-style-type: none"> PathSSL patch encoder which is based on ViT-S architecture and pre-trained following the approach in [87] with masked siamese networks [137] SSL scheme Q-Former from BLIP-2 [138] as WSI-encoder Among two variants PathAlign-R and PathAlign-G, PathAlign-G uses PaLM-2 S [139] as the frozen LLM 	<ul style="list-style-type: none"> In-house de-identified dataset (DS1) of WSIs paired with reports collected from a teaching hospital. The stain type for the WSIs are H&E and IHC TCGA 	<ul style="list-style-type: none"> Performs WSI classification, image-to-text retrieval and text generation 	—
MI-Gen [57]	<ul style="list-style-type: none"> ResNet and ViT (ImageNet initialization or hierarchical SSPT with HIPT [140]) as visual encoder CNN layer in the hierarchical position-aware module (PAM) Transformer as encoder-decoder (both vanilla transformer and Mem-Transformer [141]). Additionally, CNN-RNN [142] and att-LSTM [143] is used for comparison 	PathText dataset which was created using and WSI and pathology report from TCGA-BRCA	<ul style="list-style-type: none"> Performs pathology report generation from WSI Additionally performs cancer subtyping and biomarker prediction Develops a hierarchical position-aware module (PAM) Introduces PathText dataset which contains 9,009 WSI-text pairs 	✓
W2T [49]	<ul style="list-style-type: none"> ResNet-50, ViT-S pre-trained with DINO or scheme followed in HIPT as visual encoders to extract patch features Text Encoders: PubMedBERT and BioClinicalBERT Co-attention mapping in the decoder to align visual and text features 	WSI-VQA	<ul style="list-style-type: none"> Curates a WSI VQA dataset called WSI-VQA with 977 WSIs and 8,672 Q/A Performs VQA with the proposed WSI-VQA dataset Co-attention mapping between word embeddings and WSIs are used for interpretability 	✓
PathGen-CLIP [51]	<ul style="list-style-type: none"> OpenCLIP framework is utilized to train a pathology-specific CLIP model The vision encoder of LLaVA v1.5 is replaced with the trained pathology-specific CLIP model PathGen-CLIP is combined with Vicuna LLM 	<ul style="list-style-type: none"> PathGen-1.6M (for pre-training) PatchCamelyon (Pcam) CRC-100K SICAPv2 BACH Osteo SkinCancer LC25000 Camelyon 16 and 17 	<ul style="list-style-type: none"> Curates a large-scale dataset PathGen-1.6M with 1.6 million image-caption pairs Develops a pathology-specific large multi-modal modal with the capability to adapt to various downstream task 	✓
Quilt-Net [52]	<ul style="list-style-type: none"> CLIP model (based on OpenCLIP framework) ViT-B as the image encoder GPT-2 and PubMedBERT as text encoder 	<ul style="list-style-type: none"> Quilt-1M (for pre-training) PatchCamelyon (PCam) NCT-CRC-HE-100K SICAPv2 DatabioX BACH Osteo Renal Cell SkinCancer MHIST LC25000 	<ul style="list-style-type: none"> Curates a large-scale dataset Quilt-1M Performs zero-shot, linear-probing task and also cross-modal retrieval task Provides cross-modal attention mask with Grad-CAM 	✓
Guevara et al. [144]	<ul style="list-style-type: none"> CLIP model HIPT as image encoder A transformer encoder to project encoded image embedding to match the dimension of text embedding PubMedBERT as text encoder For the caption model pre-trained Bio GPT 2 is used GPT-3.5-turbo [145] to clean and refine captions. Additionally, the captions were machine-translated from two languages to English using the approach in [146] 	Self-curated dataset of WSIs and captions. WSIs are of colon polyps and biopsies. The captions contain possible 5 diagnostic labels normal, hyperplasia, low-grade dysplasia, high-grade dysplasia, or adenocarcinoma	<ul style="list-style-type: none"> Performs WSI classification and caption generation through the use of weakly supervised transformer-based models 	—
Hu et al. [147]	<ul style="list-style-type: none"> ResNet-50 pre-trained with BYOL [148] SSL scheme as patch encoder Anchor-based module as WSI encoder based on [149] which uses kernel attention transformer Prompt-based text encoder which utilizes self-attention structure in BERT [150] 	<ul style="list-style-type: none"> GastricADC In-house gastric dataset containing 3598 WSIs and reports dataset 	<ul style="list-style-type: none"> Performs cross-modal retrieval tasks which includes image-to-image retrieval, image-to-text retrieval, text-to-image retrieval and text-to-text retrieval Proposes a histopathology language-image representation learning framework Develops a prompt-based text representation learning scheme 	✓
PEMP [151]	<ul style="list-style-type: none"> CLIP as the backbone of the proposed model A self-attention layer A attention pooling layer 	<ul style="list-style-type: none"> In-house datasets TCGA-CESC 	<ul style="list-style-type: none"> Performs survival analysis, metastasis detection and cancer subtype classification Proposes a mechanism to introduce vision and text prior knowledge in the designed prompts (both static and learnable) at both patch and slide levels Develops a self-attention layer called a lightweight messenger and an attention pooling layer called summary layer 	—
HistoCap [152] and HistoCapBERT	<ul style="list-style-type: none"> ResNet-18 to encode thumbnail image LSTM decoder according to [143] as caption generator Pre-trained HIPT encoder for WSI encoding Trainable attention layer after HIPT encoder In HistoCapBERT the LSTM decoder is replaced by a Bioclinical-BERT 	Dataset from Genotype-Tissue Expression (GTEx) portal	<ul style="list-style-type: none"> Performs caption generation given a thumbnail image and a WSI image 	✓
PathCap [153]	<ul style="list-style-type: none"> ResNet-18 to encode thumbnail image ResNet-18 to encode WSI patches Trainable attention layer after the ResNet-18 used to encode WSI patches LSTM as caption generation module 	Dataset from Genotype-Tissue Expression (GTEx) portal	<ul style="list-style-type: none"> Performs caption generation of histopathology images using multi-scale view (thumbnail of WSIs and WSIs) 	✓
Elbedwehy et al. [154]	<ul style="list-style-type: none"> Vision encoders include VGG [155], ResNet, PVT [156], Swin-Large [133], ConvNext-Large [59] Language decoders and pre-trained word embedding models include LSTM, RNN, Bi-directional RNN, BioLinkBERT-Large [157] 	PatchGastric	<ul style="list-style-type: none"> Performs caption generation of WSIs 	—
PromptBio [158]	<ul style="list-style-type: none"> PLIP as coarse-grained pathology instance classifier which filters out patches given a patch and a prompt (keeps patches associated with cancer-associated stroma) IBML [159] to encode patches followed by a fully-connected layer GPT-4 to generate pathology descriptions Series of transformer and MLP layer which performs biomarker prediction 	<ul style="list-style-type: none"> TCGA-CRC The Clinical Proteomic Tumor Analysis Consortium (CPTAC) CRC dataset 	<ul style="list-style-type: none"> Performs biomarker prediction 	✓

Model	Architecture and Utilized Models/Frameworks	Dataset	Contribution	Availability
SGMT [160]	<ul style="list-style-type: none"> ResNet-18 (pre-trained on ImageNet) as patch encoder Transformer encoder to encode the patch features Transformer decoder as caption generation module 	PatchGastric	<ul style="list-style-type: none"> Performs caption generation of WSIs Proposes a novel mechanism to use subtype prediction as a guiding mechanism for the caption generation task Develops a random sampling and voting strategy to select patches 	—
Tsuneki et al. [117]	<ul style="list-style-type: none"> EfficientNetB3 [161] and DenseNet121 [162] (pre-trained on ImageNet) as image encoder Average and global pooling layer after the image encoders RNN decoder layer for caption generation 	PatchGastric	<ul style="list-style-type: none"> Performs caption generation of WSIs Curates a captioned dataset of 262,777 patches from 991 WSIs 	✓

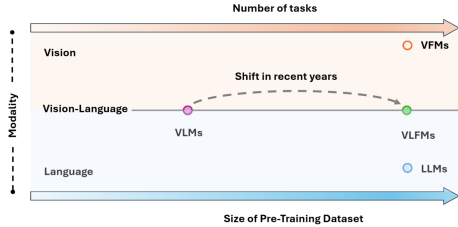


Fig. 17. Visualization of categorization of VLMs and VLFMs. There are no clear distinctive criteria for a model to be classified as a VLFM or a VLM.

VLMs and VLFMs should be viewed as a spectrum where if the number of tasks and pre-training data size increases it moves away from VLMs and towards VLFMs.

TABLE IX
SUMMARY OF PRE-TRAINING STRATEGIES IN VLMs

Strategy	Reference
Performs pre-training from scratch (vision or language module)	[52], [51]
Utilize domain-specific vision module (HIPT, CTransPath, etc) or language module (PubMedBERT, BioClinicalBERT, etc)	[158], [152], [147], [144], [49], [57], [134]
Initialize with out-of-domain encoders (ImageNet pre-training, pre-trained CLIP, etc)	[117], [160], [154], [119]

Owing to this, some VLMs follow the FM approach of pre-training the vision or text module. However, as pre-training from scratch requires a large amount of data and computing some VLMs use domain-specific vision modules from HIPT, CTransPath, IBMIL, etc or language modules from PubMedBERT, BioClinicalBERT, etc. This allows the vision or language module to learn an initial vision or language representation space which might not be as rich as pre-training scratch but boosts the performance. A summary of the choice of encoder type and pre-training strategy is provided in Table IX.

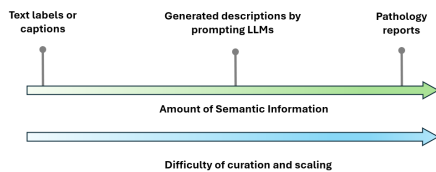


Fig. 18. Amount of semantic information available through different text sources.

Another categorization can be done by analyzing how language prior is incorporated into the model. Most works

use text labels or captions curated from different sources, which provide the least amount of information. Recent works like FSWC [113], ViLA-MIL [114] and PEMP [151] utilize prompting LLMs to increase the amount of semantic information that can be gained from text labels or captions. They prompt the LLMs to generate descriptions about a particular class label or of morphological or textural patterns about patches. On the other end of the spectrum is research work utilizing all information from pathology reports which contain a lot of details. However, as shown in Fig. 18 the difficulty of curation and doing it at a scale to match the pathologist level also increases.

B. Architectural components for VLMs in CPath

Even though there is a huge variety of vision and language modules used in VLMs, it is possible to identify common structures. In Fig. 19 the common architectural components used in different stages are outlined. In the pre-processing stage, LLMs like GPT-4, GPT-3.5, GPT-3.5-turbo and GPT-3 are used to clean and refine captions or prompting them to generate descriptions. Examples of research work utilizing LLMs in the pre-processing phase include HistGen, FSWC, ViLA-MIL, FiVE, CPLIP and PromptBio.

Another key component of the architecture is the vision module or encoder which converts the WSI patches to image embeddings. As shown in Fig. 19 it can be separated into three separate groups. The first group is vanilla CNNs that have ImageNet initialization or some kind of pre-training on pathology data. Note that most VLMs utilizing these architectures are not recent works (with the exception of Elbedwehy et al. [154]). Recent VLMs utilize ViTs which is the second group containing several ViT variants. The third group is special encoders that are pathology domain-specific and optimized for encoding WSI patches. These are ideal for learning a rich representation without the cost of pre-training from scratch.

For language encoders, most works utilize BERT (PubMedBERT, BioClinicalBERT) or GPT (BioGPT, GPT 2) variants and most are pre-trained on datasets from the biomedical domain.

Another type of language module is the caption/text generation module which rather than encoding text into embedding, generates text sequences. Earlier works included RNN, LSTM and Transformer decoders and recent works include LLMs.

The most common vision-language alignment or fusion module is the CLIP model and its variations. However, some works come up with custom approaches to align vision and language representations.

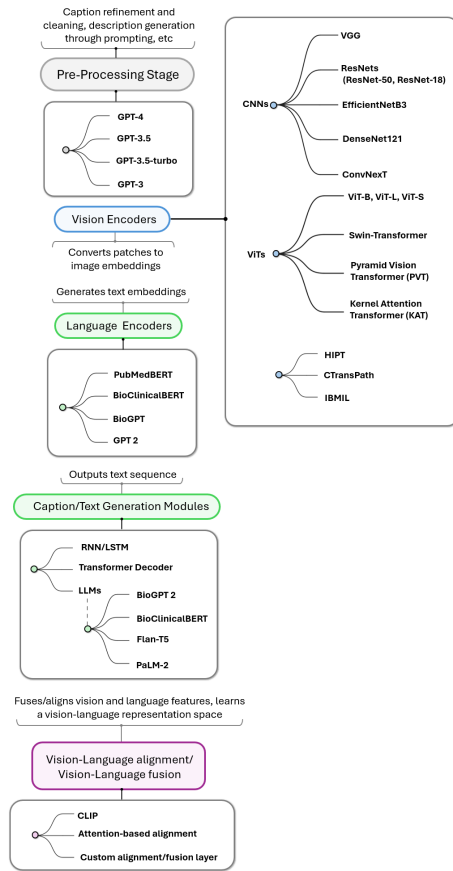


Fig. 19. Common modules used in different stages of VLMs. The last stage is the vision-language alignment or fusion stage where the vision and language embeddings generated from the earlier stages are combined.

C. Visual Instruction Tuning in CPath

There are four research works/models that fall in this category (PA-LLaVA [163], PathInsight [164], CLOVER [165], PathGen-LLaVA [51] and Quilt-LLaVA [56]).

In PA-LLaVA, a domain-specific large language-vision assistant is proposed which is a LLaVA-based model. In terms of architecture, PLIP is used as the vision encoder and LLaMA3 is used as the LLM (in conjunction with LoRA [124]). A connector module that consists of self-attention and cross-attention blocks is leveraged to project image embeddings to match the dimension of language tokens. PathInsight leverages three different multi-modal models LLaVA, Qwen-VL [166] and InternLM [167] (in conjunction with LoRA or full-parameter tuning). As the vision encoder either ViT or CLIP is used. CLOVER [165] proposes a framework for cost-effective instruction learning in CPath. It utilizes Quilt-1M as the vision-language dataset, BLIP-2 [138] for vision-language pre-training and a frozen visual encoder (EVA-ViT-G/14 [168]) and a frozen LLM (FlanT5 [116] or Vicuna [54]). The next work PathGen-LLaVA replaces the vision encoder for the CLIP model in LLaVA-v1.5 with PathGen-CLIP and as the frozen LLM Vicuna is used. The last work in this category Quilt-LLaVA is initialized with the general-domain LLaVA. Then it is tuned with QUILT for histopathological domain-alignment and finally, Quilt-instruct is used for visual

instruction tuning.

D. Related works for VLMs in CPath

There are several research works that do not directly utilize VLMs to solve a task in the pathology domain, but investigate or use VLMs for other reasons. One example is Thota et al [169] which investigates the effect of projected gradient descent (PGD) adversarial perturbation attack on PLIP [42] architecture. Another work by Lucassen et al. [170] provides a pathology report processing workflow that can be used for VLMs in CPath.

Another category of VLMs in CPath that does not directly solve pathology-specific tasks is text-guided diffusion models for image generation. However, these models can perform tasks like virtual stain transfer which can later be used to solve a pathology-specific task. Another use case is extending dataset size with generated synthetic images. One such work is PathLDM [171], that performs text-to-image generation on the TCGA-BRCA dataset.

V. CONCLUSION

In recent years the number of research works in CPath with FMs and VLMs has increased significantly which provides an indication about how CPath will evolve in the next couple of years. Many of these works put significant computing resources into training FMs on massive pre-training datasets or coming up with novel strategies to push more language prior knowledge into VLMs. In the near future, the VLFMs which bring together the benefits of both FMs and VLMs, are going to be the dominant model. This review article provides a comprehensive overview of all these models which will aid future researchers.

REFERENCES

- [1] C. L. Srinidhi, O. Ciga, and A. L. Martel, "Deep neural network models for computational histopathology: A survey," *Medical image analysis*, vol. 67, p. 101813, 2021.
- [2] S. Morales, K. Engan, and V. Naranjo, "Artificial intelligence in computational pathology—challenges and future directions," *Digital Signal Processing*, vol. 119, p. 103196, 2021.
- [3] A. Echle, N. T. Rindtorff, T. J. Brinker, T. Luedde, A. T. Pearson, and J. N. Kather, "Deep learning in cancer pathology: a new generation of clinical biomarkers," *British journal of cancer*, vol. 124, no. 4, pp. 686–696, 2021.
- [4] J. Van der Laak, G. Litjens, and F. Ciompi, "Deep learning in histopathology: the path to the clinic," *Nature medicine*, vol. 27, no. 5, pp. 775–784, 2021.
- [5] M. M. Abdelsamea, U. Zidan, Z. Senousy, M. M. Gaber, E. Rakha, and M. Ilyas, "A survey on artificial intelligence in histopathology image analysis," *Wiley Interdisciplinary Reviews: Data Mining and Knowledge Discovery*, vol. 12, no. 6, p. e1474, 2022.
- [6] I. Kim, K. Kang, Y. Song, and T.-J. Kim, "Application of artificial intelligence in pathology: trends and challenges," *Diagnostics*, vol. 12, no. 11, p. 2794, 2022.
- [7] A. Shmatko, N. Ghaffari Laleh, M. Gerstung, and J. N. Kather, "Artificial intelligence in histopathology: enhancing cancer research and clinical oncology," *Nature cancer*, vol. 3, no. 9, pp. 1026–1038, 2022.
- [8] A. Waqas, M. M. Bui, E. F. Glassy, I. El Naqa, P. Borkowski, A. A. Borkowski, and G. Rasool, "Revolutionizing digital pathology with the power of generative artificial intelligence and foundation models," *Laboratory Investigation*, p. 100255, 2023.

- [9] A. Asif, K. Rajpoot, S. Graham, D. Snead, F. Minhas, and N. Rajpoot, "Unleashing the potential of AI for pathology: challenges and recommendations," *The Journal of Pathology*, vol. 260, no. 5, pp. 564–577, 2023.
- [10] C. C. Atabansi, J. Nie, H. Liu, Q. Song, L. Yan, and X. Zhou, "A survey of transformer applications for histopathological image analysis: New developments and future directions," *BioMedical Engineering OnLine*, vol. 22, no. 1, p. 96, 2023.
- [11] M. Cooper, Z. Ji, and R. G. Krishnan, "Machine learning in computational histopathology: Challenges and opportunities," *Genes, Chromosomes and Cancer*, vol. 62, no. 9, pp. 540–556, 2023.
- [12] A. H. Song, G. Jaume, D. F. Williamson, M. Y. Lu, A. Vaidya, T. R. Miller, and F. Mahmood, "Artificial intelligence for digital and computational pathology," *Nature Reviews Bioengineering*, vol. 1, no. 12, pp. 930–949, 2023.
- [13] H. Xu, Q. Xu, F. Cong, J. Kang, C. Han, Z. Liu, A. Madabhushi, and C. Lu, "Vision transformers for computational histopathology," *IEEE Reviews in Biomedical Engineering*, 2023.
- [14] C. D. Bahadir, M. Omar, J. Rosenthal, L. Marchionni, B. Liechty, D. J. Pisapia, and M. R. Sabuncu, "Artificial intelligence applications in histopathology," *Nature Reviews Electrical Engineering*, vol. 1, no. 2, pp. 93–108, 2024.
- [15] C. McGenity, E. L. Clarke, C. Jennings, G. Matthews, C. Carlidge, H. Freduah-Agyemang, D. D. Stocken, and D. Treanor, "Artificial intelligence in digital pathology: a systematic review and meta-analysis of diagnostic test accuracy," *npj Digital Medicine*, vol. 7, no. 1, p. 114, 2024.
- [16] M. S. Hosseini, B. E. Bejnordi, V. Q.-H. Trinh, L. Chan, D. Hasan, X. Li, S. Yang, T. Kim, H. Zhang, T. Wu *et al.*, "Computational pathology: a survey review and the way forward," *Journal of Pathology Informatics*, p. 100357, 2024.
- [17] S. Brussee, G. Buzzanca, A. M. Schrader, and J. Kers, "Graph neural networks in histopathology: Emerging trends and future directions," *arXiv preprint arXiv:2406.12808*, 2024.
- [18] M. Gadermayr and M. Tschuchnig, "Multiple instance learning for digital pathology: A review of the state-of-the-art, limitations & future potential," *Computerized Medical Imaging and Graphics*, p. 102337, 2024.
- [19] J. Cheng, "Applications of large language models in pathology," *Bioengineering*, vol. 11, no. 4, p. 342, 2024.
- [20] J. N. Weinstein, E. A. Collisson, G. B. Mills, K. R. Shaw, B. A. Ozenberger, K. Ellrott, I. Shmulevich, C. Sander, and J. M. Stuart, "The cancer genome atlas pan-cancer analysis project," *Nature genetics*, vol. 45, no. 10, pp. 1113–1120, 2013.
- [21] Y. Kang, Y. J. Kim, S. Park, G. Ro, C. Hong, H. Jang, S. Cho, W. J. Hong, D. U. Kang, J. Chun *et al.*, "Development and operation of a digital platform for sharing pathology image data," *BMC Medical Informatics and Decision Making*, vol. 21, pp. 1–8, 2021.
- [22] E. Zimmermann, E. Vorontsov, J. Viret, A. Casson, M. Zelechowski, G. Shaikovski, N. Tenenholtz, J. Hall, T. Fuchs, N. Fusi *et al.*, "Virchow 2: Scaling self-supervised mixed magnification models in pathology," *arXiv preprint arXiv:2408.00738*, 2024.
- [23] S. Hua, F. Yan, T. Shen, L. Ma, and X. Zhang, "PathoDuet: Foundation models for pathological slide analysis of H&E and IHC stains," *Medical Image Analysis*, vol. 97, p. 103289, 2024.
- [24] E. Vorontsov, A. Bozkurt, A. Casson, G. Shaikovski, M. Zelechowski, K. Severson, E. Zimmermann, J. Hall, N. Tenenholtz, N. Fusi *et al.*, "A foundation model for clinical-grade computational pathology and rare cancers detection," *Nature Medicine*, pp. 1–12, 2024.
- [25] C. Saillard, R. Jenatton, F. Llinares-López, Z. Mariet, D. Cahané, E. Durand, and J.-P. Vert, "H-optimus-0," 2024. [Online]. Available: <https://github.com/biopathus/releases/tree/main/models/h-optimus/v0>
- [26] J. Dippel, B. Feulner, T. Winterhoff, S. Schallenberg, G. Dernbach, A. Kunft, S. Tietz, P. Jurmeister, D. Horst, L. Ruff *et al.*, "RudolfV: a foundation model by pathologists for pathologists," *arXiv preprint arXiv:2401.04079*, 2024.
- [27] D. Nechaev, A. Pchelnikov, and E. Ivanova, "Hibou: A family of foundational vision transformers for pathology," *arXiv preprint arXiv:2406.05074*, 2024.
- [28] Z. Yang, T. Wei, Y. Liang, X. Yuan, R. Gao, Y. Xia, J. Zhou, Y. Zhang, and Z. Yu, "A foundation model for generalizable cancer diagnosis and survival prediction from histopathological images," *bioRxiv*, pp. 2024–05, 2024.
- [29] D. Juyal, H. Padigela, C. Shah, D. Shenker, N. Harguindeguy, Y. Liu, B. Martin, Y. Zhang, M. Nercessian, M. Markey *et al.*, "PLUTO: Pathology-universal transformer," *arXiv preprint arXiv:2405.07905*, 2024.
- [30] X. Zhou, X. Zhang, C. Wu, Y. Zhang, W. Xie, and Y. Wang, "Knowledge-enhanced visual-language pretraining for computational pathology," *arXiv preprint arXiv:2404.09942*, 2024.
- [31] R. J. Chen, T. Ding, M. Y. Lu, D. F. Williamson, G. Jaume, A. H. Song, B. Chen, A. Zhang, D. Shao, M. Shaban *et al.*, "Towards a general-purpose foundation model for computational pathology," *Nature Medicine*, vol. 30, no. 3, pp. 850–862, 2024.
- [32] G. Campanella, C. Vanderbilt, and T. Fuchs, "Computational pathology at health system scale—self-supervised foundation models from billions of images," in *AAAI 2024 Spring Symposium on Clinical Foundation Models*, 2024.
- [33] A. Filiot, R. Ghermi, A. Olivier, P. Jacob, L. Fidon, A. Mac Kain, C. Saillard, and J.-B. Schiratti, "Scaling self-supervised learning for histopathology with masked image modeling," *medRxiv*, pp. 2023–07, 2023.
- [34] M. Kang, H. Song, S. Park, D. Yoo, and S. Pereira, "Benchmarking self-supervised learning on diverse pathology datasets," in *Proceedings of the IEEE/CVF Conference on Computer Vision and Pattern Recognition*, 2023, pp. 3344–3354.
- [35] X. Wang, S. Yang, J. Zhang, M. Wang, J. Zhang, W. Yang, J. Huang, and X. Han, "Transformer-based unsupervised contrastive learning for histopathological image classification," *Medical image analysis*, vol. 81, p. 102559, 2022.
- [36] J. Ma, Z. Guo, F. Zhou, Y. Wang, Y. Xu, Y. Cai, Z. Zhu, C. Jin, Y. L. X. Jiang, A. Han *et al.*, "Towards a generalizable pathology foundation model via unified knowledge distillation," *arXiv preprint arXiv:2407.18449*, 2024.
- [37] M. Y. Lu, B. Chen, D. F. Williamson, R. J. Chen, M. Zhao, A. K. Chow, K. Ikemura, A. Kim, D. Pouli, A. Patel *et al.*, "A multimodal generative AI copilot for human pathology," *Nature*, pp. 1–3, 2024.
- [38] H. Xu, N. Usuyama, J. Bagga, S. Zhang, R. Rao, T. Naumann, C. Wong, Z. Gero, J. González, Y. Gu *et al.*, "A whole-slide foundation model for digital pathology from real-world data," *Nature*, pp. 1–8, 2024.
- [39] G. Shaikovski, A. Casson, K. Severson, E. Zimmermann, Y. K. Wang, J. D. Kunz, J. A. Retamero, G. Oakley, D. Klimstra, C. Kanan *et al.*, "Prism: A multi-modal generative foundation model for slide-level histopathology," *arXiv preprint arXiv:2405.10254*, 2024.
- [40] Y. Sun, C. Zhu, S. Zheng, K. Zhang, L. Sun, Z. Shui, Y. Zhang, H. Li, and L. Yang, "PathAsst: A generative foundation AI assistant towards artificial general intelligence of pathology," in *Proceedings of the AAAI Conference on Artificial Intelligence*, vol. 38, no. 5, 2024, pp. 5034–5042.
- [41] M. Y. Lu, B. Chen, D. F. Williamson, R. J. Chen, I. Liang, T. Ding, G. Jaume, I. Odintsov, L. P. Le, G. Gerber *et al.*, "A visual-language foundation model for computational pathology," *Nature Medicine*, vol. 30, no. 3, pp. 863–874, 2024.
- [42] Z. Huang, F. Bianchi, M. Yuksekogonul, T. J. Montine, and J. Zou, "A visual-language foundation model for pathology image analysis using medical twitter," *Nature medicine*, vol. 29, no. 9, pp. 2307–2316, 2023.
- [43] J. Gui, T. Chen, J. Zhang, Q. Cao, Z. Sun, H. Luo, and D. Tao, "A survey on self-supervised learning: Algorithms, applications, and future trends," *IEEE Transactions on Pattern Analysis and Machine Intelligence*, 2024.
- [44] J. Zhang, J. Huang, S. Jin, and S. Lu, "Vision-language models for vision tasks: A survey," *IEEE Transactions on Pattern Analysis and Machine Intelligence*, 2024.
- [45] A. Radford, J. W. Kim, C. Hallacy, A. Ramesh, G. Goh, S. Agarwal, G. Sastry, A. Askell, P. Mishkin, J. Clark *et al.*, "Learning transferable visual models from natural language supervision," in *International conference on machine learning*. PMLR, 2021, pp. 8748–8763.
- [46] S. Zhang, Y. Xu, N. Usuyama, H. Xu, J. Bagga, R. Tinn, S. Preston, R. Rao, M. Wei, N. Valluri *et al.*, "BiomedCLIP: a multimodal biomedical foundation model pretrained from fifteen million scientific image-text pairs," *arXiv preprint arXiv:2303.00915*, 2023.
- [47] G. Jaume, A. Vaidya, R. J. Chen, D. F. Williamson, P. P. Liang, and F. Mahmood, "Modeling dense multimodal interactions between biological pathways and histology for survival prediction," in *Proceedings of the IEEE/CVF Conference on Computer Vision and Pattern Recognition*, 2024, pp. 11 579–11 590.
- [48] D. Ahméd-Aristizabal, M. A. Armin, S. Denman, C. Fookes, and L. Petersson, "A survey on graph-based deep learning for computational histopathology," *Computerized Medical Imaging and Graphics*, vol. 95, p. 102027, 2022.
- [49] P. Chen, C. Zhu, S. Zheng, H. Li, and L. Yang, "WSI-VQA: Interpreting whole slide images by generative visual question answering," *arXiv preprint arXiv:2407.05603*, 2024.

- [50] J. Achiam, S. Adler, S. Agarwal, L. Ahmad, I. Akkaya, F. L. Aleman, D. Almeida, J. Altenschmidt, S. Altman, S. Anadkat *et al.*, “GPT-4 technical report,” *arXiv preprint arXiv:2303.08774*, 2023.
- [51] Y. Sun, Y. Zhang, Y. Si, C. Zhu, Z. Shui, K. Zhang, J. Li, X. Lyu, T. Lin, and L. Yang, “PathGen-1.6 M: 1.6 million pathology image-text pairs generation through multi-agent collaboration,” *arXiv preprint arXiv:2407.00203*, 2024.
- [52] W. Ikezogwo, S. Seyfioglu, F. Ghezloo, D. Geva, F. Sheikh Mohammed, P. K. Anand, R. Krishna, and L. Shapiro, “Quilt-1M: One million image-text pairs for histopathology,” *Advances in neural information processing systems*, vol. 36, 2024.
- [53] H. Liu, C. Li, Q. Wu, and Y. J. Lee, “Visual instruction tuning,” *Advances in neural information processing systems*, vol. 36, 2024.
- [54] W.-L. Chiang, Z. Li, Z. Lin, Y. Sheng, Z. Wu, H. Zhang, L. Zheng, S. Zhuang, Y. Zhuang, J. E. Gonzalez, I. Stoica, and E. P. Xing, “Vicuna: An open-source chatbot impressing GPT-4 with 90%* ChatGPT quality,” March 2023. [Online]. Available: <https://lmsys.org/blog/2023-03-30-vicuna/>
- [55] G. Ilharco, M. Wortsman, R. Wightman, C. Gordon, N. Carlini, R. Taori, A. Dave, V. Shankar, H. Namkoong, J. Miller, H. Hajishirzi, A. Farhadi, and L. Schmidt, “OpenCLIP,” Jul. 2021. [Online]. Available: <https://doi.org/10.5281/zenodo.5143773>
- [56] M. S. Seyfioglu, W. O. Ikezogwo, F. Ghezloo, R. Krishna, and L. Shapiro, “Quilt-LLaVA: Visual instruction tuning by extracting localized narratives from open-source histopathology videos,” in *Proceedings of the IEEE/CVF Conference on Computer Vision and Pattern Recognition*, 2024, pp. 13 183–13 192.
- [57] P. Chen, H. Li, C. Zhu, S. Zheng, and L. Yang, “MI-Gen: Multiple instance generation of pathology reports for gigapixel whole-slide images,” *arXiv preprint arXiv:2311.16480*, 2023.
- [58] C.-Y. Wang, A. Bochkovskiy, and H.-Y. M. Liao, “YOLOv7: Trainable bag-of-freebies sets new state-of-the-art for real-time object detectors,” in *Proceedings of the IEEE/CVF conference on computer vision and pattern recognition*, 2023, pp. 7464–7475.
- [59] Z. Liu, H. Mao, C.-Y. Wu, C. Feichtenhofer, T. Darrell, and S. Xie, “A convnet for the 2020s,” in *Proceedings of the IEEE/CVF conference on computer vision and pattern recognition*, 2022, pp. 11 976–11 986.
- [60] OpenAI, “Introducing ChatGPT,” 2023, available at <https://openai.com/blog/chatgpt>.
- [61] Y. Sun, H. Wu, C. Zhu, S. Zheng, Q. Chen, K. Zhang, Y. Zhang, X. Lan, M. Zheng, J. Li *et al.*, “PathMMU: A massive multimodal expert-level benchmark for understanding and reasoning in pathology,” *arXiv preprint arXiv:2401.16355*, 2024.
- [62] C. Li, L. Li, H. Jiang, K. Weng, Y. Geng, L. Li, Z. Ke, Q. Li, M. Cheng, W. Nie *et al.*, “YOLOv6: A single-stage object detection framework for industrial applications,” *arXiv preprint arXiv:2209.02976*, 2022.
- [63] J. Redmon, S. Divvala, R. Girshick, and A. Farhadi, “You only look once: Unified, real-time object detection,” in *Proceedings of the IEEE conference on computer vision and pattern recognition*, 2016, pp. 779–788.
- [64] R. Luo, L. Sun, Y. Xia, T. Qin, S. Zhang, H. Poon, and T.-Y. Liu, “BioGPT: generative pre-trained transformer for biomedical text generation and mining,” *Briefings in bioinformatics*, vol. 23, no. 6, p. bbac409, 2022.
- [65] C. Schuhmann, R. Beaumont, R. Vencu, C. Gordon, R. Wightman, M. Cherti, T. Coombes, A. Katta, C. Mullis, M. Wortsman *et al.*, “Laion-5B: An open large-scale dataset for training next generation image-text models,” *Advances in Neural Information Processing Systems*, vol. 35, pp. 25 278–25 294, 2022.
- [66] A. Radford, J. W. Kim, T. Xu, G. Brockman, C. McLeavey, and I. Sutskever, “Robust speech recognition via large-scale weak supervision,” in *International conference on machine learning*. PMLR, 2023, pp. 28 492–28 518.
- [67] D. Doukhan, J. Carrière, F. Vallet, A. Larcher, and S. Meignier, “An open-source speaker gender detection framework for monitoring gender equality,” in *2018 IEEE international conference on acoustics, speech and signal processing (ICASSP)*. IEEE, 2018, pp. 5214–5218.
- [68] S. Nakatani, “langdetect,” <https://pypi.org/project/langdetect/>, 2015.
- [69] M. Y. Lu, B. Chen, A. Zhang, D. F. Williamson, R. J. Chen, T. Ding, L. P. Le, Y.-S. Chuang, and F. Mahmood, “Visual language pretrained multiple instance zero-shot transfer for histopathology images,” in *Proceedings of the IEEE/CVF conference on computer vision and pattern recognition*, 2023, pp. 19 764–19 775.
- [70] J. Gamper and N. Rajpoot, “Multiple instance captioning: Learning representations from histopathology textbooks and articles,” in *Proceedings of the IEEE/CVF conference on computer vision and pattern recognition*, 2021, pp. 16 549–16 559.
- [71] T. Achakulvisut, D. Acuna, and K. Kording, “Pubmed parser: A python parser for pubmed open-access xml subset and medline xml dataset xml dataset,” *Journal of Open Source Software*, vol. 5, no. 46, p. 1979, 2020. [Online]. Available: <https://doi.org/10.21105/joss.01979>
- [72] C. Clark and S. Divvala, “Pdffigures 2.0: Mining figures from research papers,” in *Proceedings of the 16th ACM/IEEE-CS on Joint Conference on Digital Libraries*, 2016, pp. 143–152.
- [73] X. He, Y. Zhang, L. Mou, E. Xing, and P. Xie, “PathVQA: 30000+ questions for medical visual question answering,” *arXiv preprint arXiv:2003.10286*, 2020.
- [74] D. Klein and C. D. Manning, “Accurate unlexicalized parsing,” in *Proceedings of the 41st annual meeting of the association for computational linguistics*, 2003, pp. 423–430.
- [75] H. Liu, C. Li, Y. Li, and Y. J. Lee, “Improved baselines with visual instruction tuning,” in *Proceedings of the IEEE/CVF Conference on Computer Vision and Pattern Recognition*, 2024, pp. 26 296–26 306.
- [76] C. Lu, H. Xu, M. Wang, D. Shi, H.-M. Qin, A. Madabhushi, P. Gao, and F. Cong, “When multiple instance learning meets foundation models: Advancing histological whole slide image analysis,” 2024.
- [77] M. Mallya, A. K. Mirabadi, H. Farahani, and A. Bashashati, “Benchmarking histopathology foundation models for ovarian cancer bevacizumab treatment response prediction from whole slide images,” *arXiv preprint arXiv:2407.20596*, 2024.
- [78] J. Lu, F. Yan, X. Zhang, Y. Gao, and S. Zhang, “PathoTune: Adapting visual foundation model to pathological specialists,” *arXiv preprint arXiv:2403.16497*, 2024.
- [79] G. Campanella, S. Chen, R. Verma, J. Zeng, A. Stock, M. Croken, B. Veremis, A. Elmas, K.-I. Huang, R. Kwan *et al.*, “A clinical benchmark of public self-supervised pathology foundation models,” *arXiv preprint arXiv:2407.06508*, 2024.
- [80] S. Zheng, X. Cui, Y. Sun, J. Li, H. Li, Y. Zhang, P. Chen, X. Jing, Z. Ye, and L. Yang, “Benchmarking PathCLIP for pathology image analysis,” *Journal of Imaging Informatics in Medicine*, pp. 1–17, 2024.
- [81] C. Yin, S. Liu, K. Zhou, V. W.-S. Wong, and P. C. Yuen, “Prompting vision foundation models for pathology image analysis,” in *Proceedings of the IEEE/CVF Conference on Computer Vision and Pattern Recognition*, 2024, pp. 11 292–11 301.
- [82] W. Aswolinskiy, M. Paulikat, and C. Aichmueller, “Impact of layer selection in histopathology foundation models on downstream task performance,” in *Medical Imaging with Deep Learning*, 2024.
- [83] N. Aben, E. D. de Jong, I. Gatopoulos, N. Känzig, M. Karasikov, A. Lagré, R. Moser, F. van Doorn, F. Tang *et al.*, “Towards large-scale training of pathology foundation models,” *arXiv preprint arXiv:2404.15217*, 2024.
- [84] D. Ferber, G. Wölflein, I. C. Wiest, M. Ligerio, S. Sainath, N. G. Laleh, O. S. El Nahhas, G. Müller-Franzes, D. Jäger, D. Truhn *et al.*, “In-context learning enables multimodal large language models to classify cancer pathology images,” *arXiv preprint arXiv:2403.07407*, 2024.
- [85] S. Alfassy, P. Nejat, S. Hemati, J. Khan, I. Lahr, A. Alsaafin, A. Shafique, N. Comfere, D. Murphree, C. Meroueh *et al.*, “Foundation models for histopathology—fanfare or flair,” *Mayo Clinic Proceedings: Digital Health*, vol. 2, no. 1, pp. 165–174, 2024.
- [86] B. Roth, V. Koch, S. J. Wagner, J. A. Schnabel, C. Marr, and T. Peng, “Low-resource finetuning of foundation models beats state-of-the-art in histopathology,” *arXiv preprint arXiv:2401.04720*, 2024.
- [87] J. Lai, F. Ahmed, S. Vijay, T. Jaroensri, J. Loo, S. Vyawahare, S. Agarwal, F. Jamil, Y. Matias, G. S. Corrado *et al.*, “Domain-specific optimization and diverse evaluation of self-supervised models for histopathology,” *arXiv preprint arXiv:2310.13259*, 2023.
- [88] A. Dosovitskiy, L. Beyer, A. Kolesnikov, D. Weissenborn, X. Zhai, T. Unterthiner, M. Dehghani, M. Minderer, G. Heigold, S. Gelly *et al.*, “An image is worth 16x16 words: Transformers for image recognition at scale,” *arXiv preprint arXiv:2010.11929*, 2020.
- [89] Z. Peng, L. Dong, H. Bao, Q. Ye, and F. Wei, “BEiT v2: Masked image modeling with vector-quantized visual tokenizers,” *arXiv preprint arXiv:2208.06366*, 2022.
- [90] O. Russakovsky, J. Deng, H. Su, J. Krause, S. Satheesh, S. Ma, Z. Huang, A. Karpathy, A. Khosla, M. Bernstein, A. C. Berg, and L. Fei-Fei, “ImageNet Large Scale Visual Recognition Challenge,” *International Journal of Computer Vision (IJCV)*, vol. 115, no. 3, pp. 211–252, 2015.
- [91] M. Caron, H. Touvron, I. Misra, H. Jégou, J. Mairal, P. Bojanowski, and A. Joulin, “Emerging properties in self-supervised vision transformers,” in *Proceedings of the IEEE/CVF international conference on computer vision*, 2021, pp. 9650–9660.
- [92] M. Oquab, T. Darcet, T. Moutakanni, H. Vo, M. Szafraniec, V. Khalidov, P. Fernandez, D. Haziza, F. Massa, A. El-Nouby *et al.*, “DINOv2:

- Learning robust visual features without supervision,” *arXiv preprint arXiv:2304.07193*, 2023.
- [93] X. Chen, H. Fan, R. Girshick, and K. He, “Improved baselines with momentum contrastive learning,” *arXiv preprint arXiv:2003.04297*, 2020.
- [94] X. Chen, S. Xie, and K. He, “An empirical study of training self-supervised vision transformers,” in *Proceedings of the IEEE/CVF international conference on computer vision*, 2021, pp. 9640–9649.
- [95] K. He, X. Chen, S. Xie, Y. Li, P. Dollár, and R. Girshick, “Masked autoencoders are scalable vision learners,” in *Proceedings of the IEEE/CVF conference on computer vision and pattern recognition*, 2022, pp. 16000–16009.
- [96] J. Zhou, C. Wei, H. Wang, W. Shen, C. Xie, A. Yuille, and T. Kong, “iBOT: Image BERT pre-training with online tokenizer,” *arXiv preprint arXiv:2111.07832*, 2021.
- [97] J. Yu, Z. Wang, V. Vasudevan, L. Yeung, M. Seyedhosseini, and Y. Wu, “CoCa: Contrastive captioners are image-text foundation models,” *arXiv preprint arXiv:2205.01917*, 2022.
- [98] L. Beyer, P. Izmailov, A. Kolesnikov, M. Caron, S. Kornblith, X. Zhai, M. Minderer, M. Tschannen, I. Alabdulmohsin, and F. Pavetic, “Flexivit: One model for all patch sizes,” in *Proceedings of the IEEE/CVF Conference on Computer Vision and Pattern Recognition*, 2023, pp. 14 496–14 506.
- [99] J. Ding, S. Ma, L. Dong, X. Zhang, S. Huang, W. Wang, N. Zheng, and F. Wei, “LongNet: Scaling transformers to 1,000,000,000 tokens,” *arXiv preprint arXiv:2307.02486*, 2023.
- [100] M. Caron, I. Misra, J. Mairal, P. Goyal, P. Bojanowski, and A. Joulin, “Unsupervised learning of visual features by contrasting cluster assignments,” *Advances in neural information processing systems*, vol. 33, pp. 9912–9924, 2020.
- [101] J. Zbontar, L. Jing, I. Misra, Y. LeCun, and S. Deny, “Barlow twins: Self-supervised learning via redundancy reduction,” in *International conference on machine learning*. PMLR, 2021, pp. 12 310–12 320.
- [102] H. Touvron, L. Martin, K. Stone, P. Albert, A. Almahairi, Y. Babaei, N. Bashlykov, S. Batra, P. Bhargava, S. Bhosale *et al.*, “Llama 2: Open foundation and fine-tuned chat models,” *arXiv preprint arXiv:2307.09288*, 2023.
- [103] A. Jaegle, F. Gimeno, A. Brock, O. Vinyals, A. Zisserman, and J. Carreira, “Perceiver: General perception with iterative attention,” in *International conference on machine learning*. PMLR, 2021, pp. 4651–4664.
- [104] A. Radford, J. Wu, R. Child, D. Luan, D. Amodei, I. Sutskever *et al.*, “Language models are unsupervised multitask learners,” *OpenAI blog*, vol. 1, no. 8, p. 9, 2019.
- [105] K. He, H. Fan, Y. Wu, S. Xie, and R. Girshick, “Momentum contrast for unsupervised visual representation learning,” in *Proceedings of the IEEE/CVF conference on computer vision and pattern recognition*, 2020, pp. 9729–9738.
- [106] Y. Wang, W.-L. Chao, K. Q. Weinberger, and L. Van Der Maaten, “SimpleShot: Revisiting nearest-neighbor classification for few-shot learning,” *arXiv preprint arXiv:1911.04623*, 2019.
- [107] I. Gatopoulos, N. Känzig, R. Moser, S. Otálora *et al.*, “eva: Evaluation framework for pathology foundation models,” in *Medical Imaging with Deep Learning*, 2024.
- [108] Y. Xu, Y. Wang, F. Zhou, J. Ma, S. Yang, H. Lin, X. Wang, J. Wang, L. Liang, A. Han *et al.*, “A multimodal knowledge-enhanced whole-slide pathology foundation model,” *arXiv preprint arXiv:2407.15362*, 2024.
- [109] U. Naseem, M. Khushi, and J. Kim, “Vision-language transformer for interpretable pathology visual question answering,” *IEEE Journal of Biomedical and Health Informatics*, vol. 27, no. 4, pp. 1681–1690, 2022.
- [110] Q. Jin, B. Dhingra, W. Cohen, and X. Lu, “Probing biomedical embeddings from language models,” in *Proceedings of the 3rd Workshop on Evaluating Vector Space Representations for NLP*, 2019, pp. 82–89.
- [111] S. M. Lundberg and S.-I. Lee, “A unified approach to interpreting model predictions,” *Advances in neural information processing systems*, vol. 30, 2017.
- [112] R. R. Selvaraju, M. Cogswell, A. Das, R. Vedantam, D. Parikh, and D. Batra, “Grad-CAM: Visual explanations from deep networks via gradient-based localization,” in *Proceedings of the IEEE international conference on computer vision*, 2017, pp. 618–626.
- [113] L. Qu, K. Fu, M. Wang, Z. Song *et al.*, “The rise of AI language pathologists: Exploring two-level prompt learning for few-shot weakly-supervised whole slide image classification,” *Advances in Neural Information Processing Systems*, vol. 36, 2024.
- [114] J. Shi, C. Li, T. Gong, Y. Zheng, and H. Fu, “ViLa-MIL: Dual-scale vision-language multiple instance learning for whole slide image classification,” in *Proceedings of the IEEE/CVF Conference on Computer Vision and Pattern Recognition*, 2024, pp. 11 248–11 258.
- [115] Q. Zhou, W. Zhong, Y. Guo, M. Xiao, H. Ma, and J. Huang, “PathM3: A multimodal multi-task multiple instance learning framework for whole slide image classification and captioning,” *arXiv preprint arXiv:2403.08967*, 2024.
- [116] H. W. Chung, L. Hou, S. Longpre, B. Zoph, Y. Tay, W. Fedus, Y. Li, X. Wang, M. Dehghani, S. Brahma *et al.*, “Scaling instruction-finetuned language models,” *Journal of Machine Learning Research*, vol. 25, no. 70, pp. 1–53, 2024.
- [117] M. Tsuneki and F. Kanavati, “Inference of captions from histopathological patches,” in *International Conference on Medical Imaging with Deep Learning*. PMLR, 2022, pp. 1235–1250.
- [118] X. Wang, Y. Peng, L. Lu, Z. Lu, and R. M. Summers, “TieNet: Text-image embedding network for common thorax disease classification and reporting in chest x-rays,” in *Proceedings of the IEEE conference on computer vision and pattern recognition*, 2018, pp. 9049–9058.
- [119] H. Watawana, K. Ranasinghe, T. Mahmood, M. Naseer, S. Khan, and F. S. Khan, “Hierarchical text-to-vision self supervised alignment for improved histopathology representation learning,” *arXiv preprint arXiv:2403.14616*, 2024.
- [120] C. Jiang, A. Chowdury, X. Hou, A. Kondepudi, C. Freudiger, K. Conway, S. Camelo-Piragua, D. Orringer, H. Lee, and T. Hollon, “OpenSRH: optimizing brain tumor surgery using intraoperative stimulated raman histology,” *Advances in neural information processing systems*, vol. 35, pp. 28 502–28 516, 2022.
- [121] H. Li, Y. Chen, Y. Chen, R. Yu, W. Yang, L. Wang, B. Ding, and Y. Han, “Generalizable whole slide image classification with fine-grained visual-semantic interaction,” in *Proceedings of the IEEE/CVF Conference on Computer Vision and Pattern Recognition*, 2024, pp. 11 398–11 407.
- [122] B. Li, Y. Li, and K. W. Eliceiri, “Dual-stream multiple instance learning network for whole slide image classification with self-supervised contrastive learning,” in *Proceedings of the IEEE/CVF conference on computer vision and pattern recognition*, 2021, pp. 14 318–14 328.
- [123] T. Wolf, L. Debut, V. Sanh, J. Chaumond, C. Delangue, A. Moi, P. Cistac, T. Rault, R. Louf, M. Funtowicz *et al.*, “Huggingface’s transformers: State-of-the-art natural language processing,” *arXiv preprint arXiv:1910.03771*, 2019.
- [124] E. J. Hu, Y. Shen, P. Wallis, Z. Allen-Zhu, Y. Li, S. Wang, L. Wang, and W. Chen, “LoRA: Low-rank adaptation of large language models,” *arXiv preprint arXiv:2106.09685*, 2021.
- [125] S. Javed, A. Mahmood, I. I. Ganapathi, F. A. Dharejo, N. Werghi, and M. Bennamoun, “CPLIP: Zero-shot learning for histopathology with comprehensive vision-language alignment,” in *Proceedings of the IEEE/CVF Conference on Computer Vision and Pattern Recognition*, 2024, pp. 11 450–11 459.
- [126] Z. Guo, J. Ma, Y. Xu, Y. Wang, L. Wang, and H. Chen, “HistGen: Histopathology report generation via local-global feature encoding and cross-modal context interaction,” *arXiv preprint arXiv:2403.05396*, 2024.
- [127] M. Asadi-Aghbolaghi, H. Farahani, A. Zhang, A. Akbari, S. Kim, A. Chow, S. Dane, O. C. Consortium, O. Consortium, D. G. Huntsman *et al.*, “Machine learning-driven histotype diagnosis of ovarian carcinoma: Insights from the ocean ai challenge,” *medRxiv*, pp. 2024–04, 2024.
- [128] H. Farahani, J. Boschman, D. Farnell, A. Darbandsari, A. Zhang, P. Ahmadvand, S. J. Jones, D. Huntsman, M. Köbel, C. B. Gilks *et al.*, “Deep learning-based histotype diagnosis of ovarian carcinoma whole-slide pathology images,” *Modern Pathology*, vol. 35, no. 12, pp. 1983–1990, 2022.
- [129] M. Veta, Y. J. Heng, N. Stathonikos, B. E. Bejnordi, F. Beca, T. Wollmann, K. Rohr, M. A. Shah, D. Wang, M. Rousson *et al.*, “Predicting breast tumor proliferation from whole-slide images: the TUPAC16 challenge,” *Medical image analysis*, vol. 54, pp. 111–121, 2019.
- [130] Z. Lai, Z. Li, L. C. Oliveira, J. Chauhan, B. N. Dugger, and C.-N. Chuah, “CLIPath: Fine-tune clip with visual feature fusion for pathology image analysis towards minimizing data collection efforts,” in *Proceedings of the IEEE/CVF International Conference on Computer Vision*, 2023, pp. 2374–2380.
- [131] E. Alsentz, J. R. Murphy, W. Boag, W.-H. Weng, D. Jin, T. Naumann, and M. McDermott, “Publicly available clinical BERT embeddings,” *arXiv preprint arXiv:1904.03323*, 2019.
- [132] Y. Gu, R. Tinn, H. Cheng, M. Lucas, N. Usuyama, X. Liu, T. Naumann, J. Gao, and H. Poon, “Domain-specific language model pretraining

- for biomedical natural language processing,” *ACM Transactions on Computing for Healthcare (HEALTH)*, vol. 3, no. 1, pp. 1–23, 2021.
- [133] Z. Liu, Y. Lin, Y. Cao, H. Hu, Y. Wei, Z. Zhang, S. Lin, and B. Guo, “Swin transformer: Hierarchical vision transformer using shifted windows,” in *Proceedings of the IEEE/CVF international conference on computer vision*, 2021, pp. 10012–10022.
- [134] M. Tran, P. Schmidle, S. J. Wagner, V. Koch, B. Novotny, V. Lupperger, A. Feuchtinger, A. Böhrner, R. Kaczmarczyk, T. Biedermann *et al.*, “Generating clinical-grade pathology reports from gigapixel whole slide images with HistoGPT,” *medRxiv*, pp. 2024–03, 2024.
- [135] J.-B. Alayrac, J. Donahue, P. Luc, A. Miech, I. Barr, Y. Hasson, K. Lenc, A. Mensch, K. Millican, M. Reynolds *et al.*, “Flamingo: a visual language model for few-shot learning,” *Advances in neural information processing systems*, vol. 35, pp. 23 716–23 736, 2022.
- [136] F. Ahmed, A. Sellergren, L. Yang, S. Xu, B. Babenko, A. Ward, N. Olsson, A. Mohtashamian, Y. Matias, G. S. Corrado *et al.*, “PathAlign: A vision-language model for whole slide images in histopathology,” *arXiv preprint arXiv:2406.19578*, 2024.
- [137] M. Assran, M. Caron, I. Misra, P. Bojanowski, F. Bordes, P. Vincent, A. Joulin, M. Rabbat, and N. Ballas, “Masked siamese networks for label-efficient learning,” in *European Conference on Computer Vision*. Springer, 2022, pp. 456–473.
- [138] J. Li, D. Li, S. Savarese, and S. Hoi, “BLIP-2: Bootstrapping language-image pre-training with frozen image encoders and large language models,” in *International conference on machine learning*. PMLR, 2023, pp. 19 730–19 742.
- [139] R. Anil, A. M. Dai, O. Firat, M. Johnson, D. Lepikhin, A. Passos, S. Shakeri, E. Taropa, P. Bailey, Z. Chen *et al.*, “PaLM 2 technical report,” *arXiv preprint arXiv:2305.10403*, 2023.
- [140] R. J. Chen, C. Chen, Y. Li, T. Y. Chen, A. D. Trister, R. G. Krishnan, and F. Mahmood, “Scaling vision transformers to gigapixel images via hierarchical self-supervised learning,” in *Proceedings of the IEEE/CVF Conference on Computer Vision and Pattern Recognition*, 2022, pp. 16 144–16 155.
- [141] Z. Chen, Y. Song, T.-H. Chang, and X. Wan, “Generating radiology reports via memory-driven transformer,” *arXiv preprint arXiv:2010.16056*, 2020.
- [142] O. Vinyals, A. Toshev, S. Bengio, and D. Erhan, “Show and tell: A neural image caption generator,” in *Proceedings of the IEEE conference on computer vision and pattern recognition*, 2015, pp. 3156–3164.
- [143] K. Xu, J. Ba, R. Kiros, K. Cho, A. Courville, R. Salakhudinov, R. Zemel, and Y. Bengio, “Show, attend and tell: Neural image caption generation with visual attention,” in *International conference on machine learning*. PMLR, 2015, pp. 2048–2057.
- [144] B. C. Guevara, N. Marini, S. Marchesin, W. Aswolinskiy, R.-J. Schlimbach, D. Podareanu, and F. Ciompi, “Caption generation from histopathology whole-slide images using pre-trained transformers,” in *Medical Imaging with Deep Learning, short paper track*, 2023.
- [145] L. Ouyang, J. Wu, X. Jiang, D. Almeida, C. Wainwright, P. Mishkin, C. Zhang, S. Agarwal, K. Slama, A. Ray *et al.*, “Training language models to follow instructions with human feedback,” *Advances in neural information processing systems*, vol. 35, pp. 27 730–27 744, 2022.
- [146] J. Tiedemann and S. Thottingal, “OPUS-MT—building open translation services for the world,” in *Proceedings of the 22nd annual conference of the European Association for Machine Translation*, 2020, pp. 479–480.
- [147] D. Hu, Z. Jiang, J. Shi, F. Xie, K. Wu, K. Tang, M. Cao, J. Huai, and Y. Zheng, “Histopathology language-image representation learning for fine-grained digital pathology cross-modal retrieval,” *Medical Image Analysis*, vol. 95, p. 103163, 2024.
- [148] J.-B. Grill, F. Strub, F. Altché, C. Tallec, P. Richemond, E. Buchatskaya, C. Doersch, B. Avila Pires, Z. Guo, M. Gheshlaghi Azar *et al.*, “Bootstrap your own latent: a new approach to self-supervised learning,” *Advances in neural information processing systems*, vol. 33, pp. 21 271–21 284, 2020.
- [149] Y. Zheng, J. Li, J. Shi, F. Xie, J. Huai, M. Cao, and Z. Jiang, “Kernel attention transformer for histopathology whole slide image analysis and assistant cancer diagnosis,” *IEEE Transactions on Medical Imaging*, vol. 42, no. 9, pp. 2726–2739, 2023.
- [150] J. Devlin, “BERT: Pre-training of deep bidirectional transformers for language understanding,” *arXiv preprint arXiv:1810.04805*, 2018.
- [151] L. Qu, D. Yang, D. Huang, Q. Guo, R. Luo, S. Zhang, and X. Wang, “Pathology-knowledge enhanced multi-instance prompt learning for few-shot whole slide image classification,” *arXiv preprint arXiv:2407.10814*, 2024.
- [152] S. Sengupta and D. E. Brown, “Automatic report generation for histopathology images using pre-trained vision transformers,” *arXiv preprint arXiv:2311.06176*, 2023.
- [153] R. Zhang, C. Weber, R. Grossman, and A. A. Khan, “Evaluating and interpreting caption prediction for histopathology images,” in *Machine Learning for Healthcare Conference*. PMLR, 2020, pp. 418–435.
- [154] S. Elbedwehy, T. Medhat, T. Hamza, and M. F. Alrahmawy, “Enhanced descriptive captioning model for histopathological patches,” *Multimedia Tools and Applications*, vol. 83, no. 12, pp. 36 645–36 664, 2024.
- [155] K. Simonyan, “Very deep convolutional networks for large-scale image recognition,” *arXiv preprint arXiv:1409.1556*, 2014.
- [156] W. Wang, E. Xie, X. Li, D.-P. Fan, K. Song, D. Liang, T. Lu, P. Luo, and L. Shao, “Pvt v2: Improved baselines with pyramid vision transformer,” *Computational Visual Media*, vol. 8, no. 3, pp. 415–424, 2022.
- [157] M. Yasunaga, J. Leskovec, and P. Liang, “LinkBERT: Pretraining language models with document links,” *arXiv preprint arXiv:2203.15827*, 2022.
- [158] L. Zhang, B. Yun, X. Xie, Q. Li, X. Li, and Y. Wang, “Prompting whole slide image based genetic biomarker prediction,” *arXiv preprint arXiv:2407.09540*, 2024.
- [159] T. Lin, Z. Yu, H. Hu, Y. Xu, and C.-W. Chen, “Interventional bag multi-instance learning on whole-slide pathological images,” in *Proceedings of the IEEE/CVF Conference on Computer Vision and Pattern Recognition*, 2023, pp. 19 830–19 839.
- [160] W. Qin, R. Xu, P. Huang, X. Wu, H. Zhang, and L. Luo, “What a whole slide image can tell? subtype-guided masked transformer for pathological image captioning,” *arXiv preprint arXiv:2310.20607*, 2023.
- [161] M. Tan and Q. Le, “EfficientNet: Rethinking model scaling for convolutional neural networks,” in *International conference on machine learning*. PMLR, 2019, pp. 6105–6114.
- [162] G. Huang, Z. Liu, L. Van Der Maaten, and K. Q. Weinberger, “Densely connected convolutional networks,” in *Proceedings of the IEEE conference on computer vision and pattern recognition*, 2017, pp. 4700–4708.
- [163] D. Dai, Y. Zhang, L. Xu, Q. Yang, X. Shen, S. Xia, and G. Wang, “PA-LLaVA: A large language-vision assistant for human pathology image understanding,” *arXiv preprint arXiv:2408.09530*, 2024.
- [164] X. Wu, R. Xu, P. Wei, W. Qin, P. Huang, Z. Li, and L. Luo, “Pathinsight: Instruction tuning of multimodal datasets and models for intelligence assisted diagnosis in histopathology,” *arXiv preprint arXiv:2408.07037*, 2024.
- [165] K. Chen, M. Liu, F. Yan, L. Ma, X. Shi, L. Wang, X. Wang, L. Zhu, Z. Wang, M. Zhou *et al.*, “Cost-effective instruction learning for pathology vision and language analysis,” *arXiv preprint arXiv:2407.17734*, 2024.
- [166] J. Bai, S. Bai, S. Yang, S. Wang, S. Tan, P. Wang, J. Lin, C. Zhou, and J. Zhou, “Qwen-VL: A frontier large vision-language model with versatile abilities,” *arXiv preprint arXiv:2308.12966*, 2023.
- [167] P. Zhang, X. D. B. Wang, Y. Cao, C. Xu, L. Ouyang, Z. Zhao, S. Ding, S. Zhang, H. Duan, H. Yan *et al.*, “Internlm-xcomposer: A vision-language large model for advanced text-image comprehension and composition,” *arXiv preprint arXiv:2309.15112*, 2023.
- [168] Y. Fang, W. Wang, B. Xie, Q. Sun, L. Wu, X. Wang, T. Huang, X. Wang, and Y. Cao, “Eva: Exploring the limits of masked visual representation learning at scale,” in *Proceedings of the IEEE/CVF Conference on Computer Vision and Pattern Recognition*, 2023, pp. 19 358–19 369.
- [169] P. Thota, J. Veerla, P. Guttikonda, M. S. Nasr, S. Nilzadeh, and J. M. Lubner, “Demonstration of an adversarial attack against a multimodal vision language model for pathology imaging,” in *21st IEEE International Symposium on Biomedical Imaging (ISBI 2024)*. IEEE, 2024.
- [170] R. Lucassen, T. van de Luijtgarden, S. Moonemans, W. Blokx, and M. Veta, “Preprocessing pathology reports for vision-language model development,” in *MICCAI Workshop on Computational Pathology with Multimodal Data (COMPAYL)*, 2024.
- [171] S. Yellapragada, A. Graikos, P. Prasanna, T. Kurc, J. Saltz, and D. Samaras, “PathLDM: Text conditioned latent diffusion model for histopathology,” in *Proceedings of the IEEE/CVF Winter Conference on Applications of Computer Vision*, 2024, pp. 5182–5191.